Mineralogical Magazine, August 2017, Vol. 81(4), pp. 753–779

Klaprothite, péligotite and ottohahnite, three new minerals with bidentate UO_7–SO_4 linkages from the Blue Lizard mine, San Juan County, Utah, USA

Anthony R. Kampf[1,*], Jakub Plášil[2], Anatoly V. Kasatkin[3], Joe Marty[4] and Jiří Čejka[5]

[1] Mineral Sciences Department, Natural History Museum of Los Angeles County, 900 Exposition Boulevard, Los Angeles, CA 90007, USA
[2] Institute of Physics ASCR, v.v.i., Na Slovance 1999/2, 18221 Prague 8, Czech Republic
[3] Fersman Mineralogical Museum of the Russian Academy of Sciences, Leninsky Prospekt, 18-2, 119071, Moscow, Russia
[4] 5199 East Silver Oak Road, Salt Lake City, UT 84108, USA
[5] Department of Mineralogy and Petrology, National Museum, Cirkusová 1740, 193 00, Prague 9, Czech Republic

[*Received 20 April 2016; Accepted 16 May 2016; Associate Editor: G. Diego Gatta*]

ABSTRACT

The new minerals klaprothite (IMA2015-087), $Na_6(UO_2)(SO_4)_4(H_2O)_4$, péligotite (IMA2015-088), $Na_6(UO_2)(SO_4)_4(H_2O)_4$ and ottohahnite (IMA2015-098), $Na_6(UO_2)_2(SO_4)_5(H_2O)_7 \cdot 1.5H_2O$, were found in the Blue Lizard mine, San Juan County, Utah, USA, where they occur together as secondary phases. All three minerals occur as yellowish-green to greenish-yellow crystals, are brittle with irregular fracture, have Mohs hardness of ~2½ and exhibit bright bluish-green fluorescence, and all are easily soluble in room-temperature H_2O. Only klaprothite exhibits cleavage; perfect on {100} and {001}. Quantitative energy-dispersive spectroscopy analyses yielded the empirical formulas $Na_{6.01}(U_{1.03}O_2)(S_{0.993}O_4)_4(H_2O)_4$, $Na_{5.82}(U_{1.02}O_2)(S_{1.003}O_4)_4(H_2O)_4$ and $Na_{5.88}(U_{0.99}O_2)_2(S_{1.008}O_4)_5(H_2O)_{8.5}$ for klaprothite, péligotite and ottohahnite, respectively. Their Raman spectra exhibit similar features. Klaprothite is monoclinic, $P2_1/c$, $a = 9.8271(4)$, $b = 9.7452(3)$, $c = 20.8725(15)$ Å, $\beta = 98.743(7)°$, $V = 1975.66(17)$ Å^3 and $Z = 4$. Péligotite is triclinic, $P\bar{1}$, $a = 9.81511(18)$, $b = 9.9575(2)$, $c = 10.6289(8)$ Å, $\alpha = 88.680(6)°$, $\beta = 73.990(5)°$, $\gamma = 89.205(6)°$, $V = 998.22(8)$ Å^3 and $Z = 2$. Ottohahnite is triclinic, $P\bar{1}$, $a = 9.97562(19)$, $b = 11.6741(2)$, $c = 14.2903(10)$ Å, $\alpha = 113.518(8)°$, $\beta = 104.282(7)°$, $\gamma = 91.400(6)°$, $V = 1464.59(14)$ Å^3 and $Z = 2$. The structures of klaprothite ($R_1 = 2.22\%$) and péligotite ($R_1 = 2.28\%$) both contain $[(UO_2)(SO_4)_4]^{6-}$ clusters in which one SO_4 group has a bidentate linkage with the UO_7 polyhedron; Na–O polyhedra link clusters into thick heteropolyhedral layers and link layers into frameworks; the structures differ in the configuration of Na–O polyhedra that link the layers. The structure of ottohahnite ($R_1 = 2.65\%$) contains $[(UO_2)_4(SO_4)_{10}]^{12-}$ clusters in which each UO_7 polyhedron has a bidentate linkage with one SO_4 group; Na–O polyhedra link clusters into a thin heteropolyhedral slice and also link the slices into a framework. The minerals are named for Martin Heinrich Klaproth (1743–1817), Eugène-Melchior Péligot (1811–1890) and Otto Hahn (1879–1968).

Keywords: klaprothite, péligotite, ottohahnite, new mineral, uranyl sulfate, crystal structure, Blue Lizard mine, Utah, USA.

Introduction

In the last few years, the Blue Lizard uranium mine in southeast Utah has proven to be a prolific source of new minerals, especially sodium uranyl sulfates (Table 1). To date, our investigations have yielded

*E-mail: akampf@nhm.org
https://doi.org/10.1180/minmag.2016.080.120

TABLE 1. New uranyl sulfate minerals from the Blue Lizard mine, arranged by their charge deficiency per anion (CDA), and including their molar proportions of H_2O, S and U.

Mineral	Structural formula	CDA (vu)	mol. H_2O (%)	mol. S (%)	mol. U (%)	Reference
Shumwayite*	$[(UO_2)(SO_4)(H_2O)_2]_2 \cdot H_2O$	0.10	0.56	0.22	0.22	Kampf *et al.* (2017*b*)
Plášilite	$Na(H_2O)_2[(UO_2)(SO_4)(OH)]$	0.17	0.45	0.18	0.18	Kampf *et al.* (2015*a*)
Alwilkinsite-(Y)	$Y(H_2O)_7[(UO_2)_3(SO_4)_2O(OH)_3](H_2O)_7$	0.20	0.72	0.09	0.14	Kampf *et al.* (2017*a*)
Bobcookite	$Na(H_2O)_2Al(H_2O)_6[(UO_2)_2(SO_4)_4(H_2O)_2] \cdot 8H_2O$	0.22	0.69	0.15	0.08	Kampf *et al.* (2015*b*)
Wetherillite	$Na_2(H_2O)_6(Mg,Zn)(H_2O)_6[(UO_2)_2(SO_4)_4(H_2O)_2] \cdot 4H_2O$	0.22	0.67	0.15	0.07	Kampf *et al.* (2015*b*)
Oppenheimerite	$Na_2(H_2O)_2[(UO_2)(SO_4)_2(H_2O)]$	0.22	0.38	0.25	0.13	Kampf *et al.* (2015*c*)
Ottohahnite	$Na_6(H_2O)_7[(UO_2)_2(SO_4)_5](H_2O)_2$	0.25	0.41	0.23	0.09	This study
Fermiite	$Na_4(H_2O)_3[(UO_2)(SO_4)_3]$	0.29	0.27	0.27	0.09	Kampf *et al.* (2015*c*)
Meisserite	$Na_5(SO_3OH)(H_2O)[(UO_2)(SO_4)_3]$	0.29	0.13	0.35	0.09	Plášil *et al.* (2013)
Klaprothtite	$Na_6(H_2O)_4[(UO_2)(SO_4)_4]$	0.33	0.27	0.27	0.07	This study
Péligotite	$Na_6(H_2O)_4[(UO_2)(SO_4)_4]$	0.33	0.27	0.27	0.07	This study
Bluelizardite	$Na_7Cl(H_2O)_2[(UO_2)(SO_4)_4]$	0.33	0.13	0.27	0.07	Plášil *et al.* (2014)
Belakovskiite	$Na_7(SO_3OH)(H_2O)_3[(UO_2)(SO_4)_4(H_2O)]$	0.34	0.21	0.30	0.06	Kampf *et al.* (2014)

*The type localities for shumwayite are the Giveaway-Simplot mine and the Green Lizard mine, but it has also been found at the Blue Lizard mine.
vu – valence units.

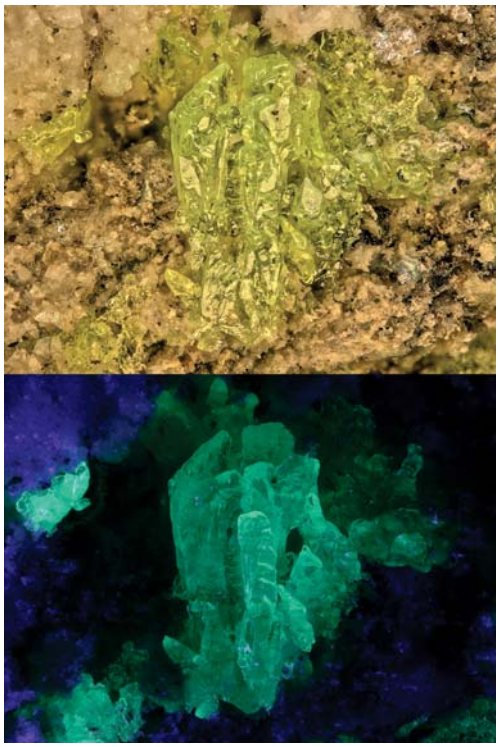

FIG. 1. Klaprothite in incandescent light (top) and in 405 nm light (bottom); field of view = 1 mm across.

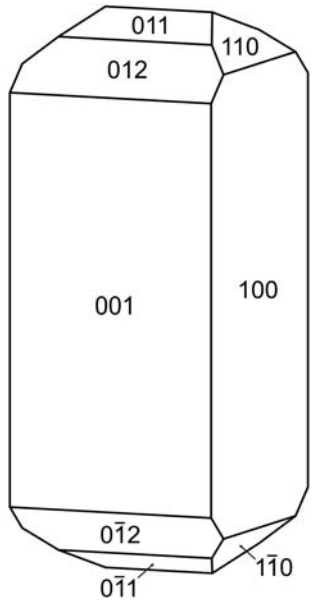

FIG. 2. Crystal drawing of klaprothite; clinographic projection in nonstandard orientation, **b** vertical.

eight new uranyl sulfate minerals, belakovskiite, bluelizardite, fermiite, meisserite, oppenheimerite, plášilite, bobcookite and wetherillite. The ninth, tenth and eleventh new uranyl sulfates from this mine, klaprothite, péligotite and ottohahnite, are described herein. These three minerals, which occur in association with one another, are the first three minerals with structures containing bidentate linkages (shared edges) between UO_7 pentagonal pyramids and SO_4 tetrahedra. The twelfth new uranyl sulfate from the Blue Lizard mine, alwilkinsite-(Y) will be described in a subsequent paper and another new one occurring here, shumwayite, was recently described from the nearby Green Lizard and Giveaway-Simplot mines.

Klaprothite (/′klæp rout ait/) is named in honour of German chemist Martin Heinrich Klaproth (1743–1817), the discoverer of uranium (1789), zirconium (1789) and cerium (1803). It should be noted that the material that Klaproth identified as a new element and named uranium was actually an oxide of the element. There have been several previous attempts to name a mineral for Klaproth, each of which subsequently resulted in a discreditation. The most recent discreditation occurred in 1947, when klaprotholite was shown to be a mixture of wittichenite and emplectite. We think that sufficient time has passed to again propose the naming a new mineral in honour of this pioneer in analytical chemistry and mineralogy.

Péligotite (/′pe li gou tait/) is named in honour of the French chemist Eugène-Melchior Péligot (1811–1890), who isolated the first sample of uranium metal in 1841 and proved that the material

FIG. 3. Péligotite with tamarugite (white); field of view = 1.1 mm across.

https://doi.org/10.1180/minmag.2016.080.120 Published online by Cambridge University Press

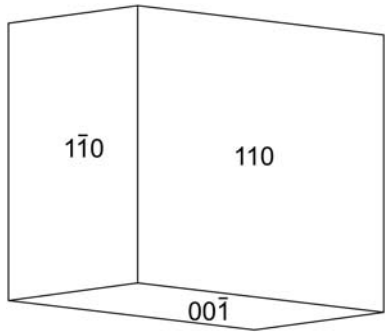

FIG. 4. Crystal drawing of péligotite; clinographic projection in standard orientation.

described by Klaproth as the element in 1789 was actually an oxide of uranium.

Ottohahnite (/au tOu ˈha:n ait/) is named in honour of German chemist Otto Hahn (1879–1968) who discovered nuclear fission (of uranium) in 1938, for which he received the Nobel Prize in Chemistry. The compound name is proposed to avoid the possible confusion of 'hahnite' with several other mineral names, i.e. hainite, gahnite and cahnite. In particular, in Russian, the pronunciation of hahnite would be essentially the same as that of gahnite.

The new minerals and their names were approved by the Commission on New Minerals, Nomenclature and Classification of the International Mineralogical Association: klaprothite (IMA2015-087), péligotite (IMA2015-088) and ottohahnite (IMA2015-098). The description of each mineral is based on five cotype specimens. Those deposited in the collections of the Natural History Museum of Los Angeles County, 900 Exposition Boulevard, Los Angeles, CA 90007, USA, have the catalogue numbers 65610 (cotype for klaprothite, péligotite and ottohahnite), 65611 (cotype for klaprothite and ottohahnite), 65612 (cotype for klaprothite), 65613 (cotype for klaprothite), 65614 (cotype for péligotite and ottohahnite), 65615 (cotype for péligotite), 65616 (cotype for péligotite) and 65617 (cotype for ottohahnite). One cotype for each mineral is housed in the collections of the Fersman Mineralogical Museum of the Russian Academy of Sciences, Moscow, Russia, registration number 4778/1 (klaprothite), 4779/1 (péligotite) and 4782/1 (ottohahnite).

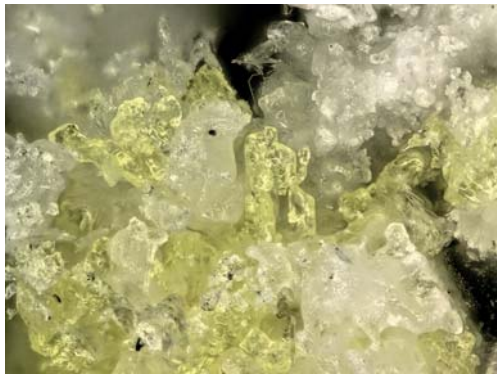

FIG. 5. Ottohahnite with tamarugite (white); field of view = 0.7 mm across.

Occurrence

Klaprothite, péligotite and ottohahnite were found underground in the Blue Lizard mine, Red Canyon, White Canyon District, San Juan County, Utah, USA (37°33′26″N 110°17′44″W). The Blue Lizard mine is located ~72 km west of the town of Blanding, Utah and ~22 km southeast of Good Hope Bay on Lake Powell. It is on the north side of Red Canyon and close to the Markey mine. Information on the history and geology of the deposit is taken largely from Chenoweth (1993).

The deposit was first recognized in the summer of 1898 by John Wetherill, while leading an archaeological expedition into Red Canyon. He noted yellow stains around a petrified tree. At that spot, he built a rock monument, in which he placed a piece of paper to claim the minerals. Although he never officially recorded his claim, 45 years later, in 1943, he described the spot to Preston V. Redd of Blanding, Utah, who went to the site, found Wetherill's monument and claimed the area as the Blue Lizzard claim (note alternate spelling). Underground workings to mine uranium were not developed until the 1950s.

Mineralized channels are in the Shinarump member of the Chinle Formation. The Shinarump member consists of medium- to coarse-grained sandstone, conglomeratic sandstone beds and thick siltstone lenses. Ore minerals were deposited as replacements of wood and other organic material and as disseminations in the enclosing sandstone. Since the mine closed in 1978, hydration-oxidation weathering of primary uranium minerals, mainly uraninite, by acidic solutions derived from the decomposition of associated sulfides such as pyrite, marcasite and chalcopyrite in the humid underground environment has produced a variety of

https://doi.org/10.1180/minmag.2016.080.120 Published online by Cambridge University Press

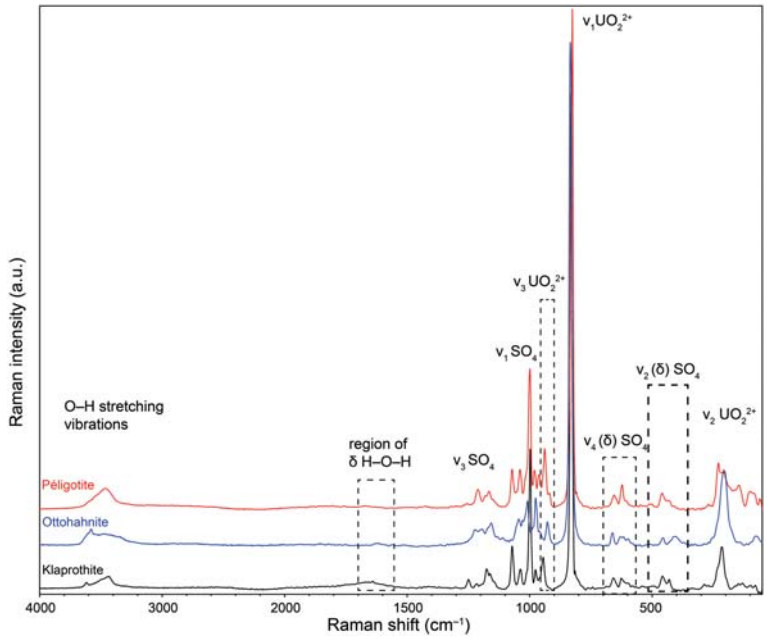

FIG. 6. The Raman spectra of klaprothite, péligotite and ottohahnite measured with a 532 nm laser.

secondary minerals, mainly sulfates, as efflorescent crusts on the surfaces of mine walls.

The new minerals are rare in the secondary uranyl sulfate mineral assemblage. Other secondary minerals found in direct association with klaprothite, péligotite and ottohahnite include blödite, bluelizardite, bobcookite, epsomite, gypsum, hexahydrite, konyaite, plášilite and tamarugite. The bulk of the matrix is comprised of subhedral to euhedral, equant quartz crystals that are recrystallized counterparts of the original grains of the sandstone. Other minerals remaining from the original sandstone include feldspar and rare almandine and zircon. Minerals related to the ore deposition include baryte, bornite, chalcopyrite, covellite, pyrite and uraninite. Other secondary minerals in the general assemblage include aluminocoquimbite, alwilkinsite-(Y), atacamite, belakovskiite, boyleite, brochantite, calcite, chalcanthite, cobaltoblödite, copiapite, coquimbite, cyanotrichite, d'ansite-(Mn), dickite, dietrichite, fermiite, ferrinatrite, gerhardtite, gordaite, halite, johannite, kaolinite, kieserite, kröhnkite, lishizhenite, manganoblödite, meisserite, metavoltine, natrozippeite, oppenheimerite, pickeringite, pseudojohannite, rhomboclase, römerite, rozenite, sideronatrite, shumwayite, thérèsemagnanite, wetherillite and other potentially new minerals currently under investigation.

A detailed discussion of the origin and conditions of formation of the uranyl sulfate assemblages at the Blue Lizard mine was provided by Plášil *et al.* (2014). The minerals formed at ambient temperature by evaporative processes at the surface of a rock with high relative porosity. The environment is relatively oxidizing (high Eh) and solutions are generally acidic (low pH). The relative acidity prevalent during the formation of any given phase can be interpreted from its charge deficiency per anion (CDA) calculated using the bond-valence approach (*cf.* Hawthorne and Schindler, 2008; Hawthorne, 2012); higher CDA correlates with higher pH. The molar proportions of S and U in the formulas are indicative of the relative concentrations of these elements in solution during formation and the molar proportion of H_2O can be expected to increase with the relative humidity (RH) during formation. Table 1 provides the CDA and molar proportions of H_2O, S and U for each of the new uranyl sulfates found at the Blue Lizard mine. Klaprothite and péligotite are likely to have formed from less acidic solutions than did ottohahnite, and most of the other uranyl sulfates at the Blue Lizard mine. Klaprothite and péligotite are presumed to have formed under relatively low RH, while ottohahnite is likely to have formed at moderate RH. The molar proportions of S and U for these

https://doi.org/10.1180/minmag.2016.080.120 Published online by Cambridge University Press

TABLE 2. Chemical analyses (in wt.%) for klaprothite, péligotite and ottohahnite.

	Klaprothite			Péligotite			Ottohahnite		
	Mean	Range	S.D.	Mean	Range	S.D.	Mean	Range	S.D.
Na_2O	21.06	19.67–22.85	1.08	20.55	18.98–22.56	1.46	13.73	12.92–15.66	0.84
UO_3	33.14	31.07–36.92	1.82	33.27	29.61–38.14	3.53	42.68	41.01–44.39	0.99
SO_3	35.93	33.15–38.40	1.38	36.60	33.88–39.20	1.88	30.44	28.86–31.45	0.97
H_2O	8.15*			8.22*			11.55§		
Total	98.28			98.64			98.40		

S.D. – standard deviation.
*Calculated by stoichiometry on the basis of 22 O apfu.
§Calculated by stoichiometry on the basis of 32.5 O apfu.

phases, with mol. S >> mol. U, suggest that they formed relatively far from the source of U (uraninite).

Physical and optical properties

Klaprothite

Klaprothite crystals are equant to prismatic (Figs 1 and 2), up to ~1 mm in maximum dimension, but usually much smaller. Crystal faces often are skeletal with rounded edges, suggestive of incomplete growth or later dissolution/deliquescence. Crystals typically occur in parallel intergrowths with surfaces made up of many stepped faces. Prisms are elongated on [010] and crystals exhibit the forms {100}, {001}, {110}, {011} and {012}. No twinning was observed.

Crystals are yellow green and transparent with a vitreous lustre. The streak is pale yellow green. The mineral fluoresces bright bluish green under both longwave and shortwave ultraviolet light. The Mohs hardness is ~2½. Crystals are brittle (slightly sectile) with perfect cleavages on {100} and {001} and have irregular fracture. The mineral is slightly deliquescent and is easily soluble in room-temperature H_2O. The density measured by flotation in a mixture of methylene iodide and acetone is 2.90(2) g cm^{-3}. The calculated densities are 2.923 g cm^{-3} based on the empirical formula and 2.905 g cm^{-3} based on the ideal formula.

Optically, klaprothite is biaxial (–) with α = 1.497(1), β = 1.517(1), γ = 1.519(1) (measured in white light). The 2V measured directly on a spindle stage is 34(1)°; the calculated 2V is 34.7°. Dispersion is $r > v$, distinct. Pleochroism is X = colourless, Y = light yellowish green, Z = light yellowish green; $X < Y \approx Z$. The optical orientation is $Y = \mathbf{b}$, $X \wedge \mathbf{c} = 10°$ in obtuse angle β.

Péligotite

Péligotite crystals are generally equant relatively simple rhombs (Figs 3 and 4), up to ~0.5 mm in maximum dimension, but usually much smaller. Crystal faces often are concave with rounded edges, suggestive of incomplete growth or later dissolution/deliquescence. Crystals typically occur in subparallel aggregates and drusy intergrowths. Crystals exhibit the forms {001}, {110} and {1$\bar{1}$0}; more complex forms are probably present, but are difficult to measure because crystals occur in tight intergrowths. No twinning was observed.

Crystals are yellow green and transparent with a vitreous lustre. The streak is pale yellow green. The mineral fluoresces bright bluish green under both longwave and shortwave ultraviolet light. The Mohs hardness is ~2½. Crystals are brittle (slightly sectile) with no cleavage and have irregular fracture. The mineral is slightly deliquescent and is easily soluble in room-temperature H_2O. The density measured by flotation in a mixture of methylene iodide and acetone is 2.88(2) g cm^{-3}. The calculated densities are 2.878 g cm^{-3} based on the empirical formula and 2.875 g cm^{-3} based on the ideal formula.

Optically, péligotite is biaxial (–) with 1.493(1), β = 1.511(1), γ = 1.515(1) (measured in white light). The 2V measured directly on a spindle stage is 50(1)°; the calculated 2V is 50.0°. Dispersion is $r > v$, distinct. Pleochroism is X = colourless, Y = light yellowish green, Z = light yellowish green; $X < Y \approx Z$. The optical orientation is $X \wedge \mathbf{c} = 3°$, $Y \wedge \mathbf{b} = 43°$, $Z \wedge \mathbf{a} = 40°$.

Ottohahnite

Ottohahnite crystals are generally equant (Fig. 5), up to ~0.1 mm in maximum dimension, but

https://doi.org/10.1180/minmag.2016.080.120 Published online by Cambridge University Press

TABLE 3. Powder X-ray data for klaprothite, péligotite and ottohahnite.

Klaprothite																							
I_{obs}	d_{obs}	d_{calc}	I_{calc}	$h\,k\,l$	I_{obs}	d_{obs}	d_{calc}	I_{calc}	$h\,k\,l$	I_{obs}	d_{obs}	d_{calc}	I_{calc}	$h\,k\,l$	I_{obs}	d_{obs}	d_{calc}	I_{calc}	$h\,k\,l$
30	10.27	10.3150	28	0 0 2	31	2.716	2.7292	19	2 2 4	16	2.0613	2.0630	13	0 0 10	11	1.6489	1.6547	3	$\bar{5}$ 1 8
68	9.72	9.7129	76	1 0 0			2.7068	4	$\bar{1}$ 3 1	10	2.0244	2.0365	4	2 4 3			1.6525	3	$\bar{4}$ 3 8
		8.8115	4	0 1 1			2.7028	3	$\bar{1}$ 3 4			2.0328	3	4 1 4			1.6455	2	4 2 7
		7.6777	7	$\bar{1}$ 0 2			2.6966	6	3 2 0			2.0261	2	$\bar{1}$ 3 8			1.6391	2	$\bar{5}$ 1 5
97	7.09	7.0838	100	0 1 2			2.6679	2	$\bar{2}$ 3 2			2.0103	2	$\bar{3}$ 3 6			1.6374	2	$\bar{1}$ 3 11
		6.8795	4	1 1 0	22	2.646	2.6657	6	3 1 3			1.9957	2	4 2 3	23	1.6233	1.6288	2	3 3 8
		6.5891	6	1 0 2			2.6545	6	$\bar{3}$ 1 5			1.9825	2	$\bar{2}$ 4 5			1.6272	6	1 1 12
		6.3250	2	1 1 1			2.6486	5	2 3 1	17	1.9504	1.9584	6	1 0 10			1.6242	3	4 1 8
36	6.04	6.0309	40	$\bar{1}$ 1 2			2.6244	4	2 0 6			1.9549	4	$\bar{3}$ 4 1			1.6232	2	2 5 5
		5.6186	3	0 1 3			2.6135	6	1 2 6			1.9404	3	0 5 1			1.6210	2	$\bar{5}$ 3 5
31	5.467	5.4585	41	1 1 2	35	2.570	2.5904	7	1 3 4	48	1.9136	1.9254	13	$\bar{5}$ 1 2			1.6188	2	6 0 0
77	5.158	5.1575	82	0 0 4			2.5787	6	0 0 8			1.9217	3	3 4 1			1.6152	2	$\bar{6}$ 1 2
28	4.835	4.8722	25	$\bar{1}$ 0 4			2.5743	9	$\bar{1}$ 2 6			1.9196	5	$\bar{3}$ 4 3	12	1.5931	1.6020	4	$\bar{3}$ 1 12
		4.8565	3	2 0 0			2.5596	7	2 3 2			1.9186	2	3 3 5			1.5943	2	3 5 3
		4.7421	11	0 2 1			2.5523	8	0 3 5			1.9165	2	$\bar{5}$ 0 4			1.5919	3	$\bar{3}$ 5 5
14	4.557	4.5585	13	0 1 4			2.5341	2	2 1 6			1.9156	3	$\bar{1}$ 2 10			1.5810	3	$\bar{4}$ 3 9
		4.3750	2	$\bar{2}$ 1 1			2.5276	2	$\bar{1}$ 3 5			1.9147	3	4 3 1	12	1.5640	1.5689	3	$\bar{1}$ 6 3
58	4.330	4.3553	32	1 2 0	17	2.500	2.5245	4	$\bar{3}$ 2 4			1.9118	2	4 2 4			1.5601	4	3 4 7
		4.3213	9	$\bar{1}$ 2 1			2.5218	4	0 2 7			1.9109	9	1 5 0	16	1.5361	1.5404	3	3 3 9
		4.2929	23	1 0 4			2.4929	8	0 1 8			1.9080	7	$\bar{1}$ 5 1			1.5392	2	$\bar{6}$ 1 6
46	4.194	4.2160	33	$\bar{2}$ 1 2			2.4797	2	$\bar{2}$ 3 4			1.8976	5	1 5 1			1.5350	2	$\bar{3}$ 3 11
		4.2038	2	1 2 1			2.4753	5	$\bar{3}$ 1 6	27	1.8751	1.8833	7	$\bar{4}$ 1 8			1.5341	2	$\bar{6}$ 2 4
		4.1571	14	2 0 2			2.4363	2	0 4 0			1.8778	5	$\bar{1}$ 4 7	11	1.5129	1.5291	2	2 1 12
		4.1411	2	2 1 1	8	2.415	2.4282	2	4 0 0			1.8752	5	$\bar{4}$ 2 7			1.5265	3	$\bar{4}$ 5 1
13	3.960	3.9757	5	0 2 3			2.4195	3	0 4 1			1.8737	4	$\bar{3}$ 0 10			1.5091	2	$\bar{2}$ 3 12
		3.9286	7	1 1 4			2.4034	2	1 0 8			1.8717	2	5 1 1	10	1.4898	1.4980	2	$\bar{4}$ 1 12
28	3.811	3.8237	17	$\bar{2}$ 1 2			2.3743	7	$\bar{4}$ 1 2			1.8702	2	4 3 2			1.4899	2	$\bar{1}$ 5 9
		3.7983	11	$\bar{1}$ 2 3	34	2.357	2.3671	4	1 2 7	17	1.8492	1.8597	8	$\bar{2}$ 2 10			1.4879	2	2 6 3
		3.7194	3	$\bar{1}$ 1 5			2.3634	9	$\bar{2}$ 1 8			1.8555	2	$\bar{1}$ 5 3			1.4848	3	0 5 9
13	3.572	3.5710	14	1 2 3			2.3613	2	0 3 6			1.8483	9	3 1 8	12	1.4687	1.4736	2	0 0 14
		3.5419	3	0 2 4			2.3576	3	$\bar{1}$ 4 1	27	1.8145	1.8298	5	3 4 3			1.4724	2	$\bar{4}$ 5 5
100	3.434	3.4537	8	$\bar{2}$ 2 1			2.3522	6	$\bar{2}$ 3 5			1.8252	6	$\bar{2}$ 3 9			1.4715	4	$\bar{2}$ 4 11
		3.4453	15	$\bar{1}$ 2 4			2.3381	7	$\bar{4}$ 0 4			1.8171	2	1 2 10			1.4645	2	$\bar{5}$ 2 10
		3.4397	68	2 2 0			2.3335	3	1 1 8			1.8133	2	$\bar{3}$ 3 8	13	1.4456	1.4508	3	6 2 7
		3.4083	5	$\bar{1}$ 0 6	19	2.303	2.3106	3	2 2 6			1.8114	9	$\bar{2}$ 4 7			1.4473	2	5 4 3
		3.3739	15	$\bar{2}$ 2 2			2.3065	6	$\bar{3}$ 3 1			1.8092	3	$\bar{5}$ 2 3			1.4467	2	1 5 9
37	3.227	3.2424	9	0 1 6			2.3030	2	4 1 1			1.8045	2	5 2 0			1.4404	2	$\bar{3}$ 6 3
		3.2376	14	3 0 0			2.2964	4	0 4 3			1.8027	3	2 0 10			1.4336	2	5 1 8
		3.2211	6	1 2 4			2.2914	3	$\bar{3}$ 3 2	16	1.7881	1.7980	5	1 3 9	17	1.4213	1.4292	2	$\bar{6}$ 3 5
		3.2172	9	$\bar{1}$ 1 6			2.2744	3	3 2 4			1.7931	3	2 5 1			1.4257	3	$\bar{1}$ 2 14
		3.2089	4	0 3 1	10	2.260	2.2657	2	$\bar{3}$ 2 6			1.7908	3	2 3 8			1.4225	2	$\bar{1}$ 6 7
		3.1625	4	2 2 2			2.2607	5	$\bar{1}$ 4 3			1.7835	4	$\bar{5}$ 2 4			1.4204	3	4 4 7
		3.1210	5	2 1 4			2.2526	4	3 3 1			1.7709	2	0 4 8			1.4158	2	3 1 12
65	3.082	3.1049	15	$\bar{3}$ 1 1	11	2.215	2.2268	6	4 1 2	16	1.7528	1.7623	5	0 5 5	10	1.4010	1.4106	4	$\bar{2}$ 2 14
		3.0966	10	1 0 6			2.2165	2	$\bar{2}$ 3 6			1.7541	4	$\bar{1}$ 5 5			1.4013	3	3 6 3
		3.0807	6	1 3 0			2.2098	4	1 4 3			1.7508	2	4 3 4			1.3929	2	1 6 7
		3.0725	5	3 1 0			2.1964	2	3 0 6			1.7488	3	$\bar{3}$ 2 10	15	1.3795	1.3893	2	$\bar{7}$ 1 2
		3.0682	38	$\bar{3}$ 1 2			2.1927	2	$\bar{4}$ 2 1			1.7337	4	4 2 6			1.3842	2	4 5 5
61	3.012	3.0257	10	1 3 1			2.1891	2	3 3 2	26	1.7159	1.7294	7	$\bar{4}$ 4 1			1.3830	2	$\bar{5}$ 1 12
		3.0154	41	$\bar{2}$ 2 4	19	2.179	2.1845	4	$\bar{3}$ 3 4			1.7199	2	4 4 0			1.3770	2	$\bar{1}$ 7 1
		2.9917	12	$\bar{1}$ 3 2			2.1812	5	$\bar{2}$ 4 1			1.7146	6	1 5 5	9	1.3531	1.3544	3	$\bar{4}$ 0 14
12	2.930	2.9518	10	2 2 3			2.1766	3	2 3 5			1.7124	6	$\bar{4}$ 4 3			1.3474	2	$\bar{7}$ 1 6
		2.9136	7	1 3 2			2.1733	3	4 2 0			1.7063	2	5 1 4	15	1.3361	1.3416	2	$\bar{4}$ 4 11
		2.8951	2	$\bar{2}$ 1 6			2.1584	4	$\bar{4}$ 2 3			1.7053	2	$\bar{4}$ 0 10			1.3406	2	$\bar{1}$ 4 13
26	2.816	2.8349	14	$\bar{3}$ 1 2			2.1429	2	$\bar{4}$ 0 6			1.6972	4	$\bar{3}$ 4 7			1.3391	4	$\bar{2}$ 7 1
		2.8248	3	$\bar{3}$ 1 4			2.1282	2	$\bar{3}$ 2 7	25	1.6852	1.6930	3	0 1 12			1.3356	2	7 1 2
		2.8210	2	0 1 7	18	2.100	2.1180	7	$\bar{2}$ 4 3			1.6922	3	$\bar{2}$ 5 5			1.3262	3	4 5 9
		2.8078	7	2 1 5			2.1080	4	$\bar{4}$ 2 4			1.6907	3	2 2 10	9	1.3166	1.3189	2	1 5 11
		2.7929	7	$\bar{1}$ 2 6			2.1028	3	$\bar{3}$ 3 5			1.6820	3	4 3 5			1.3157	2	$\bar{1}$ 7 5
		2.7622	2	1 3 3			2.0962	5	2 1 8			1.6808	2	$\bar{5}$ 3 2	11	1.2955	1.3046	2	2 2 14
							2.0929	5	$\bar{4}$ 1 6			1.6795	4	$\bar{5}$ 3 1			1.2960	2	$\bar{7}$ 1 8
							2.0834	2	$\bar{1}$ 0 10			1.6787	3	$\bar{2}$ 1 12			1.2928	2	$\bar{1}$ 1 16
																	1.2889	3	$\bar{2}$ 7 5

usually much smaller. Crystal faces and edges are often rounded, suggestive of incomplete growth or later dissolution/deliquescence. Crystals are typically intergrown with tamarugite. No crystals forms could be measured. No twinning was observed.

Crystals are green yellow and transparent with a vitreous lustre. The streak is pale green yellow. The mineral fluoresces bright bluish green under both longwave and shortwave ultraviolet light. The Mohs hardness is ~2½. Crystals are brittle (slightly sectile) with no cleavage and have irregular fracture. The mineral is slightly deliquescent and is easily soluble in room-temperature H_2O. The small size and difficulty of separating crystals from their intergrowths with tamarugite made the measurement of the density impractical. The calculated densities are 2.858 g cm^{-3} based on

https://doi.org/10.1180/minmag.2016.080.120 Published online by Cambridge University Press

TABLE 3. (*contd.*)

Péligotite																					
I_{obs}	d_{obs}	d_{calc}	I_{calc}	$h\,k\,l$	I_{obs}	d_{obs}	d_{calc}	I_{calc}	$h\,k\,l$	I_{obs}	d_{obs}	d_{calc}	I_{calc}	$h\,k\,l$	I_{obs}	d_{obs}	d_{calc}	I_{calc}	$h\,k\,l$
39	10.19	10.2146	42	0 0 1	18	2.816	2.8199	3	$\bar{1}\,\bar{1}\,3$	7	2.1394	2.1448	3	2 4 2			1.7115	4	$\bar{3}\,5\,1$
		9.9546	11	0 1 0			2.8161	14	1 3 2			2.1378	6	4 2 0	13	1.6908	1.7052	2	$\bar{4}\,4\,0$
48	9.51	9.4341	70	1 0 0			2.8083	5	0 3 2			2.1221	7	$4\,\bar{1}\,1$			1.7039	2	$0\,\bar{5}\,3$
32	8.15	8.1378	49	1 0 1			2.7966	3	$\bar{3}\,0\,1$	3	2.0958	2.0842	3	1 1 5			1.7024	2	0 0 6
100	7.11	7.2014	44	0 1 1			2.7552	7	2 3 1			2.0823	2	$\bar{1}\,2\,4$			1.6952	4	5 3 2
		7.0589	56	$0\,\bar{1}\,1$			2.7511	2	3 2 1			2.0622	3	2 1 5			1.6893	6	3 1 6
		6.8744	8	1 1 0	24	2.717	2.7295	9	2 2 3	11	2.0459	2.0429	16	0 0 5			1.6756	2	$\bar{2}\,5\,2$
		6.8209	12	$\bar{1}\,1\,0$			2.7240	5	2 3 0			2.0242	2	$\bar{2}\,0\,4$			1.6725	2	$0\,\bar{1}\,6$
		6.3716	10	1 1 1			2.7146	4	$3\,\bar{2}\,1$	9	1.9919	2.0037	3	$2\,\bar{3}\,4$	8	1.6605	1.6659	2	$\bar{5}\,2\,1$
32	6.23	6.2316	34	$1\,\bar{1}\,1$			2.7107	5	$2\,\bar{3}\,1$			2.0022	5	4 1 4			1.6636	2	$\bar{3}\,2\,4$
		6.1384	3	$\bar{1}\,0\,1$			2.6934	7	$3\,\bar{1}\,1$			1.9909	5	0 5 0			1.6555	3	$\bar{1}\,3\,5$
		5.2411	11	$\bar{1}\,1\,1$			2.6913	6	$\bar{3}\,1\,1$			1.9875	2	$\bar{4}\,2\,1$			1.6524	2	$4\,\bar{4}\,3$
		5.2088	10	$\bar{1}\,\bar{1}\,1$			2.6700	8	$2\,\bar{2}\,3$			1.9837	2	4 3 1			1.6347	2	$\bar{5}\,3\,0$
		5.1209	3	1 0 2			2.6492	2	$\bar{3}\,2\,0$			1.9656	5	4 3 2			1.6334	2	$\bar{4}\,4\,1$
63	5.14	5.1073	71	0 0 2	21	2.639	2.6450	7	3 2 2			1.9590	2	3 4 0			1.6316	2	$\bar{1}\,3\,5$
8	4.79	4.8175	8	2 0 1			2.6324	10	$3\,\bar{1}\,3$			1.9557	2	3 4 2	15	1.6235	1.6276	2	$5\,\bar{0}\,5$
43	4.54	4.5994	15	1 1 2			2.6206	10	$\bar{2}\,2\,2$			1.9535	2	$5\,\bar{0}\,2$			1.6247	2	$\bar{2}\,2\,5$
		4.5815	22	0 1 2			2.6044	4	$2\,\bar{2}\,2$			1.9516	2	$3\,\bar{1}\,5$			1.6230	5	$\bar{3}\,5\,1$
		4.5100	23	$0\,2\,1$			2.5605	2	$2\,0\,4$	26	1.9434	1.9449	20	$\bar{1}\,5\,0$			1.6208	4	$0\,2\,6$
		4.4396	2	$0\,\bar{1}\,1$	17	2.552	2.5566	6	$\bar{1}\,2\,3$			1.9409	4	$3\,\bar{3}\,2$			1.6185	2	$1\,\bar{6}\,1$
53	4.307	4.3880	22	$\bar{1}\,2\,0$			2.5537	5	0 0 4			1.9357	2	$1\,\bar{2}\,5$			1.6110	2	$1\,5\,4$
		4.3663	2	2 1 1			2.5508	3	$\bar{1}\,3\,2$			1.9335	6	$3\,\bar{1}\,5$			1.6084	2	$\bar{5}\,1\,2$
		4.3071	2	$2\,\bar{1}\,1$			2.5434	3	$2\,\bar{3}\,2$			1.9238	2	$1\,\bar{5}\,1$			1.6056	2	$4\,3\,5$
		4.2896	13	1 2 1			2.5269	4	$\bar{2}\,3\,1$	30	1.9131	1.9229	4	3 3 4			1.6044	2	$\bar{1}\,6\,1$
		4.2757	18	2 1 0			2.4886	2	0 4 0			1.9163	7	$2\,\bar{2}\,5$	6	1.5889	1.5988	2	$6\,\bar{1}\,1$
		4.2498	11	$\bar{2}\,1\,0$	9	2.471	2.4855	6	0 1 4			1.9153	2	$\bar{4}\,3\,0$			1.5905	2	$2\,5\,4$
21	4.078	4.0689	12	2 0 2			2.4653	3	$2\,\bar{1}\,4$			1.9132	16	$5\,\bar{1}\,1$			1.5841	3	$\bar{1}\,1\,6$
		4.0485	18	$\bar{1}\,0\,2$			2.4617	4	$0\,\bar{1}\,4$			1.9101	8	$4\,\bar{1}\,2$			1.5752	2	$\bar{3}\,4\,3$
13	3.852	3.8792	4	$\bar{1}\,2\,1$			2.4509	2	4 0 1			1.8917	2	$\bar{1}\,0\,5$	7	1.5602	1.5690	3	2 6 0
		3.8530	9	$\bar{1}\,2\,1$			2.4396	3	$3\,2\,1$			1.8893	2	$\bar{1}\,4\,3$			1.5645	2	$5\,3\,1$
		3.7967	3	2 1 2			2.4291	4	0 4 1	12	1.8716	1.8879	3	$3\,2\,3$			1.5638	2	$0\,4\,5$
16	3.754	3.7667	7	$\bar{1}\,1\,2$			2.4110	2	1 4 0			1.8868	2	5 0 0			1.5604	3	$\bar{3}\,3\,4$
		3.7369	15	$2\,\bar{1}\,2$			2.4088	2	4 0 2			1.8853	2	$5\,0\,3$			1.5483	3	$\bar{3}\,3\,4$
19	3.598	3.6274	14	$\bar{2}\,1\,1$	18	2.392	2.4069	4	0 4 1			1.8684	3	$4\,2\,4$	11	1.5317	1.5424	3	$1\,3\,6$
		3.6133	3	1 2 2			2.4005	5	0 3 3			1.8670	6	$2\,2\,4$			1.5358	4	$\bar{4}\,3\,3$
		3.6007	7	0 2 2			2.3951	2	1 4 1			1.8549	3	3 4 3			1.5346	2	$\bar{4}\,0\,4$
20	3.526	3.5282	27	1 0 3			2.3921	4	$\bar{2}\,1\,3$	10	1.8430	1.8514	3	2 5 1			1.5331	2	$3\,3\,6$
		3.4921	9	2 2 1			2.3870	5	4 1 1			1.8460	3	$5\,\bar{1}\,3$			1.5243	2	$2\,\bar{6}\,2$
		3.4372	3	2 2 0			2.3806	3	$2\,\bar{1}\,3$			1.8425	2	$0\,\bar{5}\,2$			1.5171	2	$2\,0\,7$
73	3.418	3.4319	35	$2\,\bar{2}\,1$			2.3663	5	1 2 4			1.8374	2	1 4 4			1.5151	3	$\bar{4}\,1\,4$
		3.4105	28	$\bar{2}\,2\,0$	20	2.340	2.3585	4	4 0 0			1.8288	2	$2\,\bar{5}\,1$			1.4844	2	$1\,\bar{1}\,7$
		3.4049	29	0 0 3			2.3530	3	$0\,\bar{3}\,3$			1.8264	2	$5\,2\,1$	4	1.4599	1.4693	2	$\bar{4}\,2\,4$
		3.3182	6	0 3 0			2.3460	9	3 3 1			1.8190	2	$4\,\bar{3}\,1$			1.4624	3	$5\,\bar{1}\,6$
11	3.249	3.2695	8	3 0 1			2.3319	2	$4\,\bar{1}\,2$	15	1.8065	1.8134	5	$3\,\bar{4}\,3$	3	1.4307	1.4356	2	$1\,5\,5$
		3.2021	6	$0\,\bar{1}\,3$			2.3303	2	$3\,\bar{1}\,2$			1.8088	2	$5\,\bar{2}\,2$			1.4299	2	$3\,6\,3$
		3.1601	6	$\bar{1}\,2\,2$			2.3197	2	3 0 4			1.8058	6	1 3 5			1.4286	2	$\bar{6}\,2\,1$
74	3.121	3.1379	31	1 3 0			2.3119	3	$\bar{1}\,4\,1$			1.8045	2	$2\,5\,2$			1.4100	2	$\bar{2}\,2\,6$
		3.1198	40	3 1 1	11	2.279	2.3008	5	$\bar{1}\,4\,1$			1.7955	4	$\bar{1}\,5\,2$			1.4078	2	$1\,7\,0$
		3.1158	20	$2\,\bar{2}\,2$			2.2910	5	$\bar{4}\,1\,0$			1.7783	3	$\bar{1}\,2\,5$	8	1.3829	1.3922	3	$0\,\bar{4}\,6$
		3.0972	10	1 3 1			2.2816	3	3 3 2			1.7742	2	5 2 3			1.3908	2	$7\,1\,2$
		3.0840	6	3 0 2			2.2600	3	1 4 2			1.7689	2	5 2 0			1.3831	5	$\bar{1}\,5\,5$
		3.0793	6	2 1 3			2.2579	2	$\bar{1}\,1\,4$			1.7647	4	$0\,\bar{4}\,4$			1.3822	2	$4\,6\,1$
34	3.058	3.0684	6	$2\,\bar{2}\,1$			2.2547	2	$2\,2\,4$			1.7624	2	$1\,0\,6$	5	1.3578	1.3548	2	$5\,\bar{3}\,3$
		3.0650	30	$\bar{2}\,2\,1$			2.2454	2	$2\,\bar{3}\,2$	16	1.7584	1.7593	2	$3\,0\,4$			1.3471	3	$7\,1\,4$
		3.0485	6	$1\,\bar{3}\,1$	16	2.212	2.2371	8	$3\,3\,2$			1.7576	6	$4\,4\,1$	8	1.3356	1.3401	2	$5\,1\,7$
11	2.983	3.0054	13	$3\,1\,0$			2.2198	5	$0\,\bar{4}\,2$			1.7522	4	4 3 4			1.3395	2	$7\,2\,1$
		2.9919	2	$\bar{3}\,1\,0$			2.2172	3	$1\,\bar{4}\,2$			1.7473	2	$5\,1\,4$			1.3387	2	$\bar{5}\,1\,4$
		2.9625	2	$3\,1\,2$			2.2082	4	$2\,4\,0$	16	1.7263	1.7351	9	$4\,\bar{4}\,1$			1.3369	2	$7\,1\,0$
		2.9533	2	$\bar{1}\,0\,3$			2.2052	3	4 1 3			1.7338	2	$0\,5\,3$			1.3361	2	$2\,5\,6$
		2.9296	3	$3\,\bar{1}\,2$			2.1940	3	$\bar{2}\,4\,0$			1.7296	3	$\bar{3}\,1\,4$			1.3350	3	$4\,4\,6$
		2.9110	2	1 2 3			2.1876	4	$4\,\bar{2}\,1$			1.7286	3	$\bar{4}\,0\,3$			1.3342	2	$7\,\bar{2}\,3$
		2.8468	4	$1\,\bar{2}\,3$			2.1857	4	$4\,\bar{1}\,3$			1.7242	2	$\bar{3}\,4\,2$					
		2.8429	2	$\bar{1}\,1\,3$			2.1639	2	$\bar{3}\,2\,2$			1.7186	2	$2\,\bar{3}\,4$					
		2.8368	3	0 2 3			2.1535	2	$4\,\bar{2}\,2$			1.7166	4	$1\,5\,3$					

the empirical formula and 2.973 g cm^{-3} based on the ideal formula.

Optically, ottohahnite is biaxial (–) with $\alpha = 1.511(1)$, $\beta = 1.514(1)$, $\gamma = 1.537(1)$ (measured in white light). The 2V measured directly on a spindle stage is 42(2)°; the calculated 2V is 40.2°. Dispersion is $r > v$, strong. Pleochroism is X = light yellowish green, Y = colourless, Z = yellowish green; $Y < X < Z$. The optical orientation is $X \wedge \mathbf{a} = 43°$, $Y \wedge \mathbf{b} = 11°$, $Z \wedge \mathbf{c} = 29°$.

Raman spectroscopy

The Raman spectra of klaprothite, péligotite and ottohahnite were recorded on a Thermo-Scientific DXR Raman microscope interfaced to an Olympus

https://doi.org/10.1180/minmag.2016.080.120 Published online by Cambridge University Press

TABLE 3. (*contd.*)

Ottohahnite																	
I_{obs}	d_{obs}	d_{calc}	I_{calc}	$h\,k\,l$	I_{obs}	d_{obs}	d_{calc}	I_{calc}	$h\,k\,l$	I_{obs}	d_{obs}	d_{calc}	I_{calc}	$h\,k\,l$			
12	12.67	12.5801	10	0 0 1			3.3808	4	2 0 2			2.2322	2	4 $\bar{2}$ 1			
3	10.64	10.6016	2	0 1 0			3.2077	3	1 $\bar{3}$ 3	6	2.198	2.2136	3	$\bar{1}$ $\bar{5}$ 4			
		10.5726	2	0 $\bar{1}$ 1	35	3.156	3.1607	23	$\bar{2}$ 2 2			2.1935	2	$\bar{3}$ 4 0			
10	9.54	9.5744	10	1 0 0			3.1410	4	$\bar{3}$ $\bar{1}$ 1			2.1900	2	$\bar{1}$ 4 2			
7	8.92	8.9150	11	$\bar{1}$ 0 1	31	3.088	3.1023	22	$\bar{2}$ $\bar{2}$ 4	29	2.122	2.1405	2	$\bar{3}$ $\bar{4}$ 4			
32	7.64	7.6513	27	$\bar{1}$ 1 0			3.0984	2	2 $\bar{3}$ 1			2.1312	6	2 $\bar{1}$ 5			
		7.4672	6	$\bar{1}$ $\bar{1}$ 1			3.0831	2	0 3 1			2.1269	2	$\bar{2}$ 4 2			
41	6.81	6.8221	20	0 1 1			3.0651	4	$\bar{1}$ $\bar{3}$ 4			2.1248	3	$\bar{3}$ $\bar{1}$ 6			
		6.7990	11	0 $\bar{1}$ 2			3.0489	3	$\bar{2}$ 0 4			2.1234	2	1 2 4			
		6.7766	3	1 $\bar{1}$ 1	63	2.977	2.9948	4	$\bar{3}$ $\bar{1}$ 3			2.1203	3	0 5 0			
		6.7616	4	1 0 1			2.9923	2	1 $\bar{1}$ 4			2.1058	4	4 1 1			
		6.6621	5	1 1 0			2.9861	17	1 1 3			2.0931	2	$\bar{2}$ $\bar{5}$ 3			
100	6.21	6.2047	100	$\bar{1}$ $\bar{1}$ 2			2.9798	2	$\bar{2}$ $\bar{3}$ 3	10	2.071	2.0682	6	$\bar{3}$ $\bar{3}$ 6			
27	5.28	5.3008	12	0 2 0			2.9763	15	3 $\bar{1}$ 1	9	2.0106	2.0140	2	$\bar{2}$ 3 4			
		5.2863	15	0 $\bar{2}$ 2			2.9670	2	2 $\bar{3}$ 2			2.0095	2	$\bar{4}$ 3 2			
		5.0567	2	1 $\bar{1}$ 2			2.9456	4	3 1 0			1.9882	2	$\bar{2}$ $\bar{3}$ 7			
19	4.992	5.0333	11	1 $\bar{2}$ 1			2.9431	15	2 $\bar{2}$ 3	10	1.9642	1.9774	3	$\bar{1}$ $\bar{1}$ 7			
		4.9591	2	$\bar{2}$ 0 1	42	2.913	2.9176	14	0 $\bar{4}$ 2			1.9754	2	0 2 5			
		4.9338	8	$\bar{1}$ $\bar{2}$ 1			2.9078	15	2 2 1			1.9477	2	$\bar{5}$ $\bar{1}$ 3			
39	4.650	4.6894	7	1 0 2			2.8579	4	$\bar{3}$ $\bar{2}$ 2			1.9377	2	4 $\bar{1}$ 3			
		4.6826	11	$\bar{1}$ 1 2			2.8399	2	$\bar{1}$ $\bar{2}$ 5	35	1.9076	1.9146	2	1 $\bar{6}$ 3			
		4.6268	6	0 1 2	16	2.795	2.8180	2	$\bar{1}$ $\bar{1}$ 5			1.9135	8	4 $\bar{4}$ 1			
		4.6148	7	0 $\bar{1}$ 3			2.7910	2	2 0 3			1.9104	2	$\bar{5}$ 1 3			
		4.6086	4	$\bar{2}$ 1 0			2.7850	3	1 3 1			1.9088	9	0 4 3			
		4.5296	7	$\bar{2}$ $\bar{1}$ 1			2.7727	4	0 2 3			1.9020	4	0 $\bar{4}$ 7			
24	4.465	4.4575	14	$\bar{2}$ 0 2			2.7644	2	0 $\bar{2}$ 5			1.8815	2	$\bar{3}$ $\bar{5}$ 3			
		4.3875	2	1 2 0	5	2.660	2.6558	2	3 1 1	23	1.8604	1.8752	3	3 $\bar{5}$ 3			
		4.3796	2	$\bar{2}$ $\bar{1}$ 2			2.6447	2	0 3 2			1.8687	3	$\bar{4}$ $\bar{4}$ 3			
15	4.301	4.3096	10	$\bar{1}$ 0 3			2.5385	2	3 $\bar{3}$ 1			1.8624	2	$\bar{1}$ $\bar{6}$ 2			
		4.2539	2	$\bar{1}$ 2 1	10	2.513	2.5284	2	2 $\bar{2}$ 4			1.8593	4	1 5 1			
18	4.153	4.1934	3	0 0 3			2.5160	4	0 0 5			1.8553	4	$\bar{4}$ 0 6			
		4.1529	8	2 1 0			2.4824	3	$\bar{4}$ 0 1			1.8399	2	1 $\bar{2}$ 7			
		4.1084	6	2 0 1	10	2.456	2.4679	4	$\bar{2}$ 4 0	12	1.7895	1.8074	2	$\bar{5}$ $\bar{2}$ 1			
		3.8466	2	0 $\bar{3}$ 1			2.4316	2	$\bar{1}$ 4 1			1.7914	3	$\bar{1}$ 3 5			
		3.8301	2	$\bar{2}$ 1 3			2.4301	2	$\bar{3}$ 1 4			1.7851	3	$\bar{5}$ 3 1			
12	3.802	3.8048	6	1 $\bar{1}$ 3	11	2.402	2.4257	2	1 $\bar{3}$ 5			1.7693	2	4 2 2			
		3.6405	2	1 2 1			2.4029	2	$\bar{4}$ 1 2			1.7491	2	2 0 6			
12	3.558	3.5916	3	$\bar{1}$ 3 2			2.3992	4	$\bar{1}$ 2 4	8	1.7343	1.7375	5	$\bar{2}$ 6 0			
		3.5339	2	0 3 0			2.3813	3	$\bar{3}$ $\bar{3}$ 1	13	1.7021	1.7154	3	$\bar{3}$ 5 2			
		3.5242	4	0 $\bar{3}$ 3			2.3587	2	$\bar{2}$ $\bar{4}$ 1			1.7113	2	$\bar{5}$ $\bar{3}$ 5			
52	3.462	3.4917	3	$\bar{1}$ 3 1	11	2.294	2.3017	3	$\bar{3}$ 3 2			1.7083	4	$\bar{2}$ 6 6			
		3.4750	32	$\bar{1}$ 3 0			2.2871	2	4 $\bar{1}$ 1			1.6962	3	2 $\bar{6}$ 5			
		3.4440	3	$\bar{1}$ $\bar{2}$ 4			2.2775	2	$\bar{2}$ 3 3			1.6904	2	4 0 4			
		3.4316	3	0 $\bar{1}$ 4	13	2.255	2.2586	3	$\bar{4}$ $\bar{1}$ 4								
							2.2539	5	3 0 3								

Only calculated lines with $I > 2$ are shown.
The data in these three tables are also deposited with the Principal Editor of *Mineralogical Magazine* and are available from http://www.minersoc.org/pages/e_journals/dep_mat_mm.html.

microscope (objective 50×). The spectrometer was calibrated by a software-controlled calibration procedure (within *Omnic 8* software) using multiple neon emission lines (wavelength calibration), multiple polystyrene Raman bands (laser frequency calibration), and standardized white light sources (intensity calibration). Spectral manipulation such as background correction and band-component analysis was done with *Omnic 8* software. Spectra of all three minerals are displayed in Fig. 6.

OH stretching and H_2O bending vibrations

The bands attributable to the O–H stretching vibrations were observed for all three minerals, in

https://doi.org/10.1180/minmag.2016.080.120 Published online by Cambridge University Press

TABLE 4. Data collection and structure refinement details for klaprothite, péligotite and ottohahnite.

	Klaprothite	Péligotite	Ottohahnite
Structural formula	$Na_6(UO_2)(SO_4)_4(H_2O)_4$	$Na_6(UO_2)(SO_4)_4(H_2O)_4$	$Na_6(UO_2)_2(SO_4)_5(H_2O)_7 \cdot 1.5H_2O$
Space group	$P2_1/c$	$P\bar{1}$	$P\bar{1}$
Unit-cell dimensions	$a = 9.8271(4)$ Å	$a = 9.81511(18)$ Å	$a = 9.97562(19)$ Å
	$b = 9.7452(3)$ Å	$b = 9.9575(2)$ Å	$b = 11.6741(2)$ Å
	$c = 20.8725(15)$ Å	$c = 10.6289(8)$ Å	$c = 14.2903(10)$ Å
	$\beta = 98.743(7)°$	$\alpha = 88.680(6)°$	$\alpha = 113.518(8)°$
		$\beta = 73.990(5)°$	$\beta = 104.282(7)°$
		$\gamma = 89.205(6)°$	$\gamma = 91.400(6)°$
V	1975.66(17) Å^3	998.22(8) Å^3	1464.59(14) Å^3
Z	4	2	2
Density (for above formula)	2.906 g·cm^{-3}	2.875 g·cm^{-3}	2.978 g·cm^{-3}
Absorption coefficient	8.877 mm^{-1}	8.784 mm^{-1}	11.611 mm^{-1}
F(000)	1624	812	1216
Crystal size (μm)	80 × 60 × 30	60 × 45 × 25	80 × 60 × 50
θ range	3.02 to 27.49°	3.20 to 27.44°	3.00 to 27.44°
Index ranges	$-12 \le h \le 12$	$-12 \le h \le 11$	$-11 \le h \le 12$
	$-12 \le k \le 12$	$-12 \le k \le 12$	$-15 \le k \le 15$
	$-27 \le l \le 27$	$-13 \le l \le 13$	$-18 \le l \le 18$
Reflections collected; unique	23,627/4507; $R_{int} = 0.035$	17,794/4512; $R_{int} = 0.039$	26,283/6658; $R_{int} = 0.041$
Reflections with $F_o > 4\sigma(F)$	4034	4146	5721
Completeness to θ_{max}	99.5%	99.1%	99.6%
Restraints/parameters	12/325	12/325	0/425
Goof	1.098	1.089	1.040
Final R indices [$F_o > 4\sigma(F)$]	$R_1 = 0.0222$, $wR_2 = 0.0455$	$R_1 = 0.0228$, $wR_2 = 0.0490$	$R_1 = 0.0265$, $wR_2 = 0.0581$
R indices (all data)	$R_1 = 0.0271$, $wR_2 = 0.0470$	$R_1 = 0.0273$, $wR_2 = 0.0506$	$R_1 = 0.0341$, $wR_2 = 0.0610$
Largest diff. peak/hole	+1.09/–0.86 e A^{-3}	+1.14/–0.67 e A^{-3}	+1.35/–1.38 e A^{-3}

*$R_{int} = \Sigma|F_o^2 - F_o^2(\text{mean})|/\Sigma[F_o^2]$. Goof = $S = \{\Sigma[w(F_o^2 - F_c^2)^2]/(n-p)\}^{1/2}$. $R_1 = \Sigma||F_o| - |F_c||/\Sigma|F_o|$. $wR_2 = \{\Sigma[w(F_o^2 - F_c^2)^2]/\Sigma[w(F_o^2)^2]\}^{1/2}$; $w = 1/[\sigma^2(F_o^2) + (aP)^2 + bP]$ where P is $[2F_c^2 + \text{Max}(F_o^2, 0)]/3$; for klaprothite a is 0.0153 and b is 5.0943; for péligotite a is 0.2090 and b is 1.0734; for ottohahnite a is 0.0288 and b is 2.1310.

TABLE 5. Atom coordinates and displacement parameters (Å^2) for klaprothite, péligotite and ottohahnite.

Klaprothite	*x/a*	*y/b*	*z/c*	U_{eq}	U^{11}	U^{22}	U^{33}	U^{23}	U^{13}	U^{12}
Na1	0.90437(17)	0.30192(16)	0.89756(8)	0.0239(3)	0.0252(8)	0.0193(8)	0.0268(8)	0.0013(7)	0.0025(6)	–0.0041(7)
Na2	0.26877(17)	0.23763(17)	0.75503(8)	0.0271(4)	0.0240(9)	0.0303(9)	0.0256(8)	–0.0052(7)	–0.0008(7)	0.0031(7)
Na3	0.30983(19)	0.22928(17)	0.99039(8)	0.0303(4)	0.0376(10)	0.0256(9)	0.0247(8)	0.0045(7)	–0.0048(7)	–0.0117(7)
Na4	0.40612(17)	0.81668(16)	0.90064(8)	0.0254(4)	0.0240(8)	0.0267(9)	0.0242(8)	–0.0004(7)	–0.0003(6)	–0.0067(7)
Na5	0.3506(2)	0.62409(19)	0.74617(9)	0.0410(5)	0.0575(13)	0.0289(10)	0.0411(11)	–0.0083(8)	0.0219(9)	–0.0097(9)
Na6	0.0	0.5	0.5	0.0325(6)	0.0346(14)	0.0409(14)	0.0241(12)	0.0123(11)	0.0115(10)	0.0166(12)
Na7	0.5	0.5	0	0.0988(19)	0.075(3)	0.163(4)	0.0460(19)	0.059(2)	–0.0328(18)	–0.092(3)
U	0.99601(2)	0.20230(2)	0.60250(2)	0.01284(4)	0.01114(7)	0.01244(7)	0.01492(7)	0.00186(5)	0.00187(4)	–0.00010(5)
S1	0.66470(9)	0.53766(9)	0.87958(4)	0.01520(18)	0.0154(4)	0.0136(4)	0.0170(4)	0.0001(3)	0.0036(3)	–0.0022(3)
S2	0.16743(10)	0.04653(9)	0.88370(4)	0.01691(18)	0.0154(4)	0.0165(4)	0.0190(4)	0.0007(4)	0.0034(3)	–0.0018(4)
S3	0.26752(9)	0.45861(9)	0.60626(4)	0.01456(18)	0.0114(4)	0.0134(4)	0.0190(4)	–0.0005(3)	0.0028(3)	–0.0004(3)
S4	0.22619(9)	0.49007(9)	0.87535(4)	0.01472(18)	0.0137(4)	0.0136(4)	0.0170(4)	–0.0004(3)	0.0026(3)	0.0013(3)
O1	0.3707(3)	0.0712(3)	0.68903(13)	0.0309(7)	0.045(2)	0.0300(17)	0.0176(14)	–0.0040(12)	0.0032(13)	0.0023(14)
O2	0.5873(3)	0.6234(3)	0.91893(13)	0.0247(6)	0.0220(15)	0.0252(15)	0.0283(15)	–0.0042(12)	0.0087(12)	0.0022(12)
O3	0.6440(3)	0.3917(3)	0.89178(14)	0.0272(6)	0.0321(17)	0.0141(13)	0.0345(16)	0.0026(12)	0.0024(13)	–0.0063(12)
O4	0.8155(3)	0.5630(3)	0.90098(15)	0.0300(7)	0.0157(15)	0.0303(16)	0.0445(18)	0.0038(14)	0.0061(13)	–0.0052(13)
O5	0.1284(4)	0.0692(4)	0.81476(15)	0.0445(9)	0.040(2)	0.071(3)	0.0219(16)	0.0061(16)	0.0023(14)	0.0007(18)
O6	0.8981(3)	0.6436(3)	0.57752(14)	0.0253(6)	0.0229(15)	0.0180(14)	0.0353(16)	0.0055(12)	0.0052(12)	–0.0015(12)
O7	0.3169(3)	0.0514(3)	0.90312(14)	0.0274(7)	0.0146(14)	0.0322(16)	0.0361(17)	–0.0025(13)	0.0068(12)	–0.0046(12)
O8	0.8771(3)	0.4064(3)	0.59786(17)	0.0354(8)	0.0303(18)	0.0149(14)	0.060(2)	–0.0011(14)	0.0026(15)	0.0069(13)
O9	0.2088(3)	0.5943(3)	0.59533(18)	0.0373(8)	0.0297(17)	0.0169(15)	0.068(2)	0.0035(15)	0.0151(16)	0.0094(13)
O10	0.3031(3)	0.4250(3)	0.67504(13)	0.0282(7)	0.0286(16)	0.0387(18)	0.0172(14)	–0.0008(12)	0.0030(12)	–0.0108(14)
O11	0.3860(3)	0.4425(3)	0.57219(13)	0.0211(6)	0.0150(13)	0.0248(14)	0.0244(14)	0.0000(12)	0.0061(11)	0.0023(11)
O12	0.1596(3)	0.3577(3)	0.57522(13)	0.0236(6)	0.0216(15)	0.0271(15)	0.0214(14)	–0.0001(12)	0.0007(11)	–0.0119(12)
O13	0.2590(3)	0.4444(3)	0.81359(14)	0.0298(7)	0.0390(18)	0.0257(15)	0.0275(15)	–0.0070(13)	0.0139(13)	0.0030(14)
O14	0.3122(3)	0.4266(3)	0.92971(14)	0.0263(6)	0.0196(15)	0.0293(16)	0.0276(15)	0.0103(12)	–0.0043(12)	–0.0002(12)
O15	0.0770(3)	0.4683(3)	0.87985(13)	0.0211(6)	0.0139(13)	0.0159(13)	0.0334(15)	–0.0014(11)	0.0035(11)	–0.0026(11)
O16	0.2383(3)	0.6437(3)	0.87958(13)	0.0198(6)	0.0149(13)	0.0117(12)	0.0339(15)	–0.0009(11)	0.0072(11)	–0.0002(10)
O17	0.0502(3)	0.2256(3)	0.68669(13)	0.0218(6)	0.0190(14)	0.0271(15)	0.0197(13)	–0.0016(11)	0.0042(11)	0.0008(12)
O18	0.9439(3)	0.1845(3)	0.51757(13)	0.0255(6)	0.0268(15)	0.0305(16)	0.0182(13)	0.0017(12)	0.0007(11)	–0.0029(13)
OW1	0.8704(4)	0.2477(6)	0.78456(18)	0.0576(12)	0.037(2)	0.106(4)	0.032(2)	–0.010(2)	0.0101(17)	–0.001(2)
H1a	0.937(5)	0.203(5)	0.783(3)	0.069						
H1b	0.880(6)	0.317(4)	0.761(3)	0.069						
OW2	0.4328(3)	0.7935(3)	0.01370(14)	0.0270(6)	0.0331(17)	0.0228(15)	0.0272(15)	0.0002(13)	0.0115(13)	0.0009(14)

(continued)

TABLE 5. (*contd.*)

Klaprothite (*contd.*)	*x/a*	*y/b*	*z/c*	U_{eq}	U^{11}	U^{22}	U^{33}	U^{23}	U^{13}	U^{12}
H2a	0.414(5)	0.869(3)	0.023(2)	0.032						
H2b	0.393(5)	0.744(4)	0.035(2)	0.032						
OW3	0.4801(3)	0.1886(3)	0.82167(13)	0.0251(6)	0.0274(16)	0.0260(16)	0.0212(14)	–0.0022(12)	0.0019(12)	–0.0053(13)
H3a	0.526(4)	0.252(4)	0.840(2)	0.030						
H3b	0.454(5)	0.143(4)	0.8493(18)	0.030						
OW4	0.4137(4)	0.8479(3)	0.78808(15)	0.0333(7)	0.0398(19)	0.0300(17)	0.0296(17)	0.0014(14)	0.0036(15)	–0.0016(15)
H4a	0.376(4)	0.903(4)	0.763(2)	0.040						
H4b	0.499(3)	0.868(5)	0.791(2)	0.040						
Péligotite										
	x/a	*y/b*	*z/c*	U_{eq}	U^{11}	U^{22}	U^{33}	U^{23}	U^{13}	U^{12}
Na1	0.0173(2)	0.21679(18)	0.78354(16)	0.0321(4)	0.0449(11)	0.0279(10)	0.0257(9)	–0.0057(7)	–0.0139(8)	0.0180(8)
Na2	0.13381(19)	0.60608(18)	0.49903(16)	0.0312(4)	0.0367(10)	0.0336(10)	0.0223(9)	–0.0064(7)	–0.0056(7)	–0.0115(8)
Na3	0.32017(19)	0.28083(18)	0.98490(17)	0.0302(4)	0.0367(10)	0.0285(10)	0.0291(9)	–0.0105(7)	–0.0152(8)	0.0145(8)
Na4	0.48329(18)	0.30651(18)	0.21999(16)	0.0290(4)	0.0303(10)	0.0307(10)	0.0298(9)	–0.0052(7)	–0.0146(7)	0.0090(8)
Na5	0.6224(2)	0.1241(2)	0.52127(18)	0.0405(5)	0.0411(11)	0.0445(12)	0.0295(10)	–0.0090(8)	0.0028(8)	–0.0229(9)
Na6	0	0.5	0	0.0255(5)	0.0246(13)	0.0317(13)	0.0201(11)	0.0046(9)	–0.0062(9)	0.0020(10)
Na7	0.5	0	0	0.0826(15)	0.084(3)	0.137(4)	0.0279(16)	–0.0204(18)	–0.0191(16)	0.089(3)
U	0.09294(2)	0.80723(2)	0.80855(2)	0.01259(5)	0.01248(8)	0.01214(8)	0.01266(7)	–0.00023(5)	–0.00267(5)	–0.00012(5)
S1	0.23359(10)	0.02517(10)	0.23419(9)	0.01805(19)	0.0154(5)	0.0173(5)	0.0218(5)	0.0013(4)	–0.0059(4)	0.0024(4)
S2	0.27155(10)	0.47726(9)	0.76028(9)	0.01702(19)	0.0156(5)	0.0146(5)	0.0201(5)	–0.0015(3)	–0.0038(4)	0.0032(4)
S3	0.15332(10)	0.45960(9)	0.21644(9)	0.01466(18)	0.0136(5)	0.0137(5)	0.0164(4)	–0.0018(3)	–0.0035(3)	–0.0008(4)
S4	0.33207(10)	0.01303(9)	0.76845(9)	0.01533(18)	0.0143(5)	0.0147(5)	0.0167(4)	–0.0023(3)	–0.0036(3)	–0.0015(4)
O1	0.2244(4)	0.0221(4)	0.3731(3)	0.0397(8)	0.049(2)	0.048(2)	0.0190(16)	0.0021(14)	–0.0037(14)	0.0052(17)
O2	0.3376(3)	0.1233(3)	0.1628(3)	0.0256(6)	0.0203(15)	0.0266(16)	0.0273(15)	0.0020(12)	–0.0022(12)	–0.0029(12)
O3	0.2676(4)	0.8920(3)	0.1791(3)	0.0364(8)	0.047(2)	0.0201(17)	0.045(2)	–0.0065(14)	–0.0165(16)	0.0092(15)
O4	0.0921(3)	0.0632(3)	0.2179(4)	0.0401(9)	0.0176(17)	0.0341(19)	0.072(3)	0.0093(17)	–0.0188(16)	0.0027(14)
O5	0.2572(4)	0.4774(3)	0.6279(3)	0.0386(8)	0.059(2)	0.038(2)	0.0192(15)	–0.0025(13)	–0.0108(15)	0.0101(17)
O6	0.1923(3)	0.3676(3)	0.8403(3)	0.0281(7)	0.0319(17)	0.0185(15)	0.0330(17)	0.0052(12)	–0.0078(13)	–0.0001(13)
O7	0.4194(3)	0.4725(3)	0.7621(4)	0.0408(9)	0.0172(17)	0.036(2)	0.071(2)	–0.0167(17)	–0.0140(16)	0.0066(14)
O8	0.2080(3)	0.6058(3)	0.8259(3)	0.0266(7)	0.0309(17)	0.0192(15)	0.0303(16)	–0.0019(12)	–0.0099(13)	0.0081(13)
O9	0.1136(3)	0.5881(3)	0.1683(3)	0.0287(7)	0.0282(17)	0.0177(15)	0.0409(18)	0.0014(13)	–0.0111(14)	0.0068(12)
O10	0.1011(3)	0.4443(3)	0.3582(3)	0.0302(7)	0.0358(18)	0.0379(19)	0.0155(14)	–0.0028(12)	–0.0042(12)	–0.0103(14)
O11	0.3065(3)	0.4391(3)	0.1685(3)	0.0242(6)	0.0130(14)	0.0239(16)	0.0367(17)	–0.0038(12)	–0.0083(12)	0.0028(12)
O12	0.0866(3)	0.3520(3)	0.1543(3)	0.0223(6)	0.0247(16)	0.0211(15)	0.0223(14)	–0.0027(11)	–0.0082(12)	–0.0068(12)

(continued)

TABLE 5. (*contd.*)

Péligotite (*contd.*)	*x/a*	*y/b*	*z/c*	U_{eq}	U^{11}	U^{22}	U^{33}	U^{23}	U^{13}	U^{12}
O13	0.4120(3)	0.0350(3)	0.6332(3)	0.0308(7)	0.0260(17)	0.0421(19)	0.0198(15)	–0.0039(13)	0.0018(12)	–0.0100(14)
O14	0.3831(3)	0.0928(3)	0.8573(3)	0.0254(6)	0.0262(16)	0.0253(16)	0.0291(16)	–0.0104(12)	–0.0144(13)	0.0019(13)
O15	0.1781(3)	0.0374(3)	0.7821(3)	0.0200(6)	0.0141(14)	0.0168(14)	0.0305(15)	0.0014(11)	–0.0085(11)	0.0001(11)
O16	0.3355(3)	0.8660(3)	0.8039(3)	0.0235(6)	0.0175(15)	0.0137(14)	0.0404(17)	0.0007(12)	–0.0099(12)	0.0003(11)
O17	0.1527(3)	0.7912(3)	0.6350(3)	0.0218(6)	0.0268(16)	0.0217(15)	0.0159(13)	–0.0011(11)	–0.0040(11)	–0.0041(12)
O18	0.9593(3)	0.1796(3)	0.0190(3)	0.0241(6)	0.0292(16)	0.0253(16)	0.0164(13)	–0.0030(11)	–0.0038(11)	–0.0017(13)
OW1	0.0212(6)	0.2052(6)	0.5629(4)	0.0723(15)	0.109(4)	0.078(3)	0.034(2)	–0.008(2)	–0.028(3)	0.044(3)
H1a	0.030(7)	0.129(3)	0.539(7)	0.087						
H1b	0.106(4)	0.233(7)	0.536(7)	0.087						
OW2	0.5681(3)	0.3171(3)	0.9800(3)	0.0285(7)	0.0239(17)	0.0277(18)	0.0301(17)	0.0024(13)	–0.0013(13)	0.0008(14)
H2a	0.588(5)	0.392(3)	0.944(5)	0.034						
H2b	0.642(4)	0.277(4)	0.961(5)	0.034						
OW3	0.3404(3)	0.6990(3)	0.3532(3)	0.0289(7)	0.0315(18)	0.0283(18)	0.0245(16)	–0.0021(13)	–0.0037(13)	0.0029(14)
H3a	0.321(5)	0.742(4)	0.294(4)	0.035						
H3b	0.403(4)	0.647(4)	0.317(4)	0.035						
OW4	0.4291(7)	0.2766(5)	0.4487(4)	0.0841(18)	0.126(5)	0.081(4)	0.034(2)	0.004(2)	–0.005(3)	0.052(3)
H4a	0.359(5)	0.303(7)	0.510(6)	0.101						
H4b	0.486(7)	0.342(7)	0.454(8)	0.101						

Ottohahnite	*x/a*	*y/b*	*z/c*	U_{eq}	U^{11}	U^{22}	U^{33}	U^{23}	U^{13}	U^{12}
U1	0.76518(2)	0.92310(2)	0.59278(2)	0.01693(6)	0.01595(10)	0.01423(9)	0.01643(9)	0.00435(7)	0.00092(7)	0.00139(7)
U2	0.43880(2)	0.47704(2)	0.20323(2)	0.01589(5)	0.01530(10)	0.01535(9)	0.01348(8)	0.00398(7)	0.00148(7)	0.00216(7)
S1	0.64717(12)	0.22386(10)	0.18552(9)	0.0213(3)	0.0182(6)	0.0170(5)	0.0233(6)	0.0042(5)	0.0036(5)	0.0043(5)
S2	0.74046(12)	0.58141(10)	0.43301(8)	0.0173(2)	0.0161(6)	0.0153(5)	0.0150(5)	0.0029(4)	0.0011(4)	0.0015(4)
S3	0.42597(12)	0.80033(10)	0.39688(9)	0.0180(2)	0.0164(6)	0.0160(5)	0.0164(5)	0.0043(4)	–0.0003(4)	0.0041(4)
S4	0.01287(13)	0.99886(11)	0.79367(9)	0.0228(3)	0.0211(6)	0.0225(6)	0.0176(5)	0.0052(5)	–0.0016(5)	0.0036(5)
S5	0.86118(12)	0.63587(11)	0.93924(9)	0.0214(2)	0.0182(6)	0.0210(6)	0.0189(5)	0.0064(4)	–0.0012(5)	–0.0023(5)
Na1	0.8619(2)	0.28948(17)	0.81894(15)	0.0293(5)	0.0302(12)	0.0235(10)	0.0255(10)	0.0055(8)	0.0013(9)	0.0041(9)
Na2	0.5133(2)	0.33816(19)	0.41652(16)	0.0312(5)	0.0337(12)	0.0311(11)	0.0323(11)	0.0166(9)	0.0093(9)	0.0046(9)
Na3	0.0619(2)	0.6873(2)	0.61423(17)	0.0344(5)	0.0444(14)	0.0287(11)	0.0371(12)	0.0165(9)	0.0174(10)	0.0182(10)
Na4	0.8728(2)	0.1325(2)	0.02411(18)	0.0390(5)	0.0364(13)	0.0345(12)	0.0441(13)	0.0218(10)	–0.0008(10)	–0.0028(10)
Na5	0.6421(3)	0.8889(2)	0.02774(19)	0.0401(6)	0.0458(14)	0.0238(11)	0.0443(13)	0.0058(10)	0.0160(11)	0.0064(10)

(continued)

TABLE 5. (*contd.*)

Ottohahnite (*contd.*)	*x/a*	*y/b*	*z/c*	U_{eq}	U^{11}	U^{22}	U^{33}	U^{23}	U^{13}	U^{12}
O3	0.6328(5)	0.2402(4)	0.2889(3)	0.0503(12)	0.071(3)	0.059(3)	0.045(2)	0.033(2)	0.033(2)	0.028(2)
O4	0.5596(4)	0.3102(3)	0.1485(3)	0.0324(9)	0.033(2)	0.0294(19)	0.0307(19)	0.0100(16)	0.0048(16)	0.0193(16)
O5	0.8601(4)	0.5142(3)	0.4276(3)	0.0337(9)	0.029(2)	0.033(2)	0.040(2)	0.0154(17)	0.0095(17)	0.0177(17)
O6	0.6499(4)	0.5452(3)	0.4854(3)	0.0314(8)	0.032(2)	0.036(2)	0.0237(18)	0.0104(16)	0.0064(16)	–0.0033(17)
O7	0.6615(4)	0.5619(3)	0.3236(2)	0.0258(8)	0.0211(18)	0.0326(19)	0.0181(16)	0.0086(14)	0.0003(14)	–0.0040(15)
O8	0.7937(4)	0.7186(3)	0.4916(3)	0.0312(8)	0.035(2)	0.0154(16)	0.0300(19)	–0.0014(14)	0.0043(16)	0.0025(15)
O9	0.3898(4)	0.7619(4)	0.4731(3)	0.0409(10)	0.031(2)	0.061(3)	0.037(2)	0.031(2)	0.0046(17)	0.000(2)
O10	0.4102(4)	0.6908(3)	0.2950(3)	0.0333(9)	0.042(2)	0.0164(17)	0.0274(18)	0.0001(14)	0.0009(17)	0.0086(16)
O11	0.3319(4)	0.8863(3)	0.3723(3)	0.0364(9)	0.037(2)	0.0284(19)	0.038(2)	0.0119(17)	0.0023(17)	0.0173(17)
O12	0.5713(4)	0.8642(3)	0.4383(3)	0.0295(8)	0.0222(19)	0.0328(19)	0.0256(18)	0.0115(15)	–0.0047(15)	–0.0036(15)
O13	0.1514(4)	0.0527(4)	0.8109(3)	0.0450(11)	0.021(2)	0.042(2)	0.062(3)	0.019(2)	–0.0029(19)	–0.0038(18)
O14	0.9971(5)	0.9828(4)	0.8860(3)	0.0468(11)	0.062(3)	0.056(3)	0.032(2)	0.027(2)	0.015(2)	0.023(2)
O15	0.9695(4)	0.8768(3)	0.6967(3)	0.0306(9)	0.031(2)	0.0190(17)	0.0269(18)	0.0028(14)	–0.0058(15)	0.0099(15)
O16	0.9052(3)	0.0764(3)	0.7644(3)	0.0250(8)	0.0218(18)	0.0180(16)	0.0242(17)	0.0028(14)	–0.0022(14)	0.0049(14)
O17	0.9285(4)	0.6428(3)	0.0433(3)	0.0287(8)	0.0247(19)	0.035(2)	0.0229(17)	0.0145(15)	–0.0020(15)	–0.0024(16)
O18	0.0473(4)	0.3070(4)	0.0998(3)	0.0418(10)	0.039(2)	0.051(2)	0.032(2)	0.0154(19)	0.0073(18)	–0.0171(19)
O19	0.7297(4)	0.6946(3)	0.9403(3)	0.0326(9)	0.026(2)	0.0208(17)	0.0309(19)	–0.0012(15)	–0.0059(16)	0.0053(15)
O20	0.8068(3)	0.5023(3)	0.8604(3)	0.0235(7)	0.0138(16)	0.0215(16)	0.0266(17)	0.0049(14)	0.0001(14)	0.0025(13)
O21	0.8678(4)	0.9717(3)	0.5275(3)	0.0296(8)	0.026(2)	0.0302(19)	0.0319(19)	0.0116(16)	0.0104(16)	0.0011(16)
O22	0.6598(4)	0.8690(3)	0.6539(3)	0.0302(8)	0.0245(19)	0.037(2)	0.0274(18)	0.0136(16)	0.0039(15)	0.0010(16)
O23	0.4849(4)	0.5240(3)	0.1106(3)	0.0286(8)	0.028(2)	0.037(2)	0.0225(17)	0.0142(15)	0.0058(15)	0.0061(16)
O24	0.3923(3)	0.4298(3)	0.2963(3)	0.0265(8)	0.0201(18)	0.0322(19)	0.0268(18)	0.0150(15)	0.0020(14)	–0.0026(15)
OW1	0.7096(5)	0.9473(4)	0.9026(3)	0.0545(12)	0.050(3)	0.062(3)	0.041(2)	0.015(2)	0.010(2)	–0.015(2)
OW2	0.9016(4)	0.5982(4)	0.6761(3)	0.0448(11)	0.036(2)	0.064(3)	0.035(2)	0.022(2)	0.0098(18)	0.003(2)
OW3	0.7482(4)	0.2485(4)	0.9332(3)	0.0381(9)	0.038(2)	0.044(2)	0.035(2)	0.0197(18)	0.0096(18)	0.0092(19)
OW4	0.9939(5)	0.3217(4)	0.7067(3)	0.0489(11)	0.059(3)	0.046(2)	0.040(2)	0.017(2)	0.014(2)	–0.003(2)
OW5	0.1271(4)	0.7924(4)	0.5167(3)	0.0446(10)	0.038(2)	0.054(3)	0.055(3)	0.033(2)	0.018(2)	0.007(2)
OW6	0.2298(4)	0.5100(4)	0.9070(3)	0.0369(9)	0.035(2)	0.043(2)	0.036(2)	0.0196(18)	0.0093(18)	0.0060(18)
OW7a*	0.5335(8)	0.802(2)	0.1177(13)	0.076(5)	0.037(4)	0.113(14)	0.091(9)	0.068(10)	0.001(4)	–0.013(5)
OW7b*	0.5358(19)	0.906(5)	0.180(3)	0.090(16)	0.034(10)	0.15(4)	0.11(3)	0.09(3)	0.004(11)	–0.018(13)
OW8	0.7656(7)	0.7849(5)	0.2689(4)	0.0800(17)	0.095(5)	0.084(4)	0.078(4)	0.045(3)	0.033(3)	0.018(3)
OW9*	0.6236(12)	0.0097(9)	0.3142(8)	0.063(3)	0.087(8)	0.050(6)	0.070(7)	0.028(5)	0.048(6)	0.019(5)

*Occupancies: OW7a: 0.69(4); OW7b: 0.31(4); OW9: 0.5

TABLE 6. Selected bond distances (Å) and angles (°) for klaprothite, péligotite and ottohahnite.

Klaprothite

Na1–O9	2.325(3)	Na4–OW2	2.345(3)	S1–O1	1.458(3)	U–O17	1.772(3)
Na1–OW1	2.390(4)	Na4–O16	2.353(3)	S1–O2	1.464(3)	U–O18	1.777(3)
Na1–O15	2.415(3)	Na4–O11	2.376(3)	S1–O3	1.464(3)	U–O12	2.301(3)
Na1–O6	2.472(3)	Na4–OW4	2.381(4)	S1–O4	1.502(3)	U–O8	2.306(3)
Na1–O18	2.479(3)	Na4–O7	2.453(3)	<S1–O>	1.472	U–O4	2.341(3)
Na1–O3	2.690(3)	Na4–O2	2.580(3)			U–O15	2.435(3)
Na1–O4	2.694(3)	<Na4–O>	2.415	S2–O5	1.449(3)	U–O16	2.456(3)
<Na1–O>	2.495			S2–O6	1.457(3)	$<U–O_{Ur}>$	1.775
		Na5–OW4	2.396(4)	S2–O7	1.464(3)	$<U–O_{eq}>$	2.368
Na2–OW3	2.366(3)	Na5–OW3	2.425(4)	S2–O8	1.502(3)		
Na2–O13	2.366(3)	Na5–O10	2.445(3)	<S2–O>	1.468		
Na2–O17	2.394(3)	Na5–OW1	2.481(5)				
Na2–O1	2.440(3)	Na5–O13	2.498(4)	S3–O9	1.447(3)		
Na2–O10	2.531(3)	Na5–O1	2.910(4)	S3–O10	1.462(3)		
Na2–O5	2.583(4)	<Na5–O>	2.526	S3–O11	1.462(3)		
<Na2–O>	2.447			S3–O12	1.518(3)		
		Na6–O6(×2)	2.464(3)	<S3–O>	1.472		
Na3–O14	2.305(3)	Na6–O12(×2)	2.470(3)				
Na3–O11	2.427(3)	Na6–O8(×2)	2.686(4)	S4–O13	1.446(3)		
Na3–O6	2.450(3)	Na6–O9(×2)	2.788(4)	S4–O14	1.447(3)		
Na3–O2	2.467(3)	<Na6–O>	2.602	S4–O15	1.498(3)		
Na3–O7	2.523(3)			S4–O16	1.503(3)		
Na3–OW2	2.553(4)	Na7–O14(×2)	2.290(3)	<S4–O>	1.474		
Na3–O12	2.613(3)	Na7–O2(×2)	2.342(3)				
<Na3–O>	2.477	Na7–OW2(×2)	2.959(3)				

Hydrogen bonds

D–H···*A*	*D*–H	H···*A*	*D*···*A*	<*D*H*A*
OW1–H1a···O5	0.79(3)	2.30(3)	3.060(6)	161(6)
OW1–H1b···O17	0.84(3)	2.61(3)	2.905(6)	102(6)
OW2–H2a···O11	0.80(3)	2.13(3)	2.914(4)	166(5)
OW2–H2b···O3	0.79(3)	2.10(3)	2.859(4)	161(5)
OW3–H3a···O3	0.83(3)	2.00(3)	2.817(4)	174(4)
OW3–H3b···O7	0.80(3)	2.08(3)	2.842(4)	159(5)
OW4–H4a···O1	0.80(3)	2.25(3)	2.987(4)	154(4)
OW4–H4b···O10	0.86(3)	2.04(3)	2.873(5)	163(5)

the approximate range 3650–3300 cm^{-1}. The bands are very broad and of low intensity. Approximate O–H···O hydrogen bond lengths inferred from the corresponding stretching wavenumbers using Libowitzky's empirical relation (Libowitzky, 1999) vary in the range >3.2–2.77 Å.

Very weak bands at ~1650 cm^{-1}, attributed to the ν_2 (δ) H–O–H bending mode of the H_2O molecules, were observed in the spectra of all three minerals. The low intensities of bands is typical of Raman spectra, in contrast to the higher intensity of ν_2 (δ) mode bands in infrared spectra.

Vibrations of SO_4 groups

The vibrations of the sulfate tetrahedra are well resolved in the spectra of all three minerals. The activated antisymmetric vibration ν_3 (SO_4) and the splitting of the degenerate modes suggest departure from the ideal T_d symmetry. The distortion of the tetrahedra due to the bidentate linkage between the SO_4 and UO_7 bipyramids is considerable (Plášil *et al.*, 2015). Multiple bands for ν_1 (SO_4) in all three spectra are indicative of symmetrically non-equivalent SO_4 groups.

https://doi.org/10.1180/minmag.2016.080.120 Published online by Cambridge University Press

TABLE 6. (*contd*.)

Péligotite

Na1–O9	2.302(3)	Na4–O11	2.342(3)	S1–O1	1.454(3)	U–O18	1.769(3)
Na1–OW1	2.340(5)	Na4–OW4	2.353(5)	S1–O3	1.459(3)	U–O17	1.785(3)
Na1–O15	2.365(3)	Na4–O16	2.422(3)	S1–O2	1.463(3)	U–O4	2.290(3)
Na1–O18	2.429(3)	Na4–O7	2.443(4)	S1–O4	1.489(3)	U–O8	2.316(3)
Na1–O6	2.501(4)	Na4–OW2	2.455(4)	<S1–O>	1.466	U–O12	2.332(3)
Na1–O3	2.932(4)	Na4–O2	2.519(3)			U–O15	2.435(3)
Na1–O4	3.004(4)	<Na4–O>	2.422	S2–O5	1.452(3)	U–O16	2.447(3)
<Na1–O>	2.553			S2–O7	1.457(3)	<U–O_{Ur}>	1.777
		Na5–O13	2.262(3)	S2–O6	1.462(3)	<U–O_{eq}>	2.364
Na2–O10	2.309(3)	Na5–OW3	2.325(4)	S2–O8	1.514(3)		
Na2–OW3	2.371(4)	Na5–O13	2.401(3)	<S2–O>	1.471		
Na2–O5	2.403(4)	Na5–O17	2.511(3)				
Na2–O17	2.408(3)	Na5–O1	2.537(4)	S3–O9	1.455(3)		
Na2–O10	2.437(4)	Na5–OW4	2.679(6)	S3–O10	1.456(3)		
Na2–OW1	2.588(5)	<Na5–O>	2.453	S3–O11	1.461(3)		
<Na2–O>	2.419			S3–O12	1.518(3)		
		Na6–O12(×2)	2.492(3)	<S3–O>	1.473		
Na3–O14	2.313(3)	Na6–O9(×2)	2.532(3)				
Na3–O6	2.378(3)	Na6–O6(×2)	2.540(3)	S4–O14	1.442(3)		
Na3–OW2	2.452(4)	Na6–O8(×2)	2.567(4)	S4–O13	1.448(3)		
Na3–O2	2.470(3)	<Na6–O>	2.533	S4–O15	1.494(3)		
Na3–O11	2.510(3)			S4–O16	1.505(3)		
Na3–O12	2.596(3)	Na7–O14(×2)	2.311(3)	<S4–O>	1.472		
Na3–O7	2.961(4)	Na7–O2(×2)	2.359(3)				
<Na3–O>	2.526	Na7–O3(×2)	2.750(3)				
		<Na7–O>	2.473				

Hydrogen bonds

D–H···*A*	*D*–H	H···*A*	*D*···*A*	<*DHA*
OW1–H1a···O1	0.80(3)	2.46(3)	3.037(6)	130(6)
OW1–H1b···none	0.85(3)			
OW2–H2a···O11	0.83(3)	2.15(3)	2.955(4)	165(4)
OW2–H2b···O3	0.80(3)	2.27(4)	2.892(5)	135(5)
OW3–H3a···O3	0.82(3)	2.06(3)	2.856(4)	165(5)
OW3–H3b···O7	0.82(3)	2.08(3)	2.893(4)	172(5)
OW4–H4a···O5	0.85(3)	2.22(3)	2.963(6)	146(7)
OW4–H4b···none	0.87(3)			

The bands located at ~1250 cm^{-1} are attributable to split triply degenerate ν_3 (SO_4) antisymmetric stretching vibrations. Raman bands located in the range ~1080 to ~960 cm^{-1} are attributable to ν_1 (SO_4) symmetric stretching vibrations. The intensities of the bands related to the symmetric stretching mode are considerably higher than those attributed to the activated antisymmetric stretching vibrations.

The medium-weak bands located at ~650 cm^{-1} are attributed to the ν_4 (δ) triply degenerated antisymmetric stretching vibrations of SO_4 tetrahedra and the bands at ~450 cm^{-1} are assigned to the split ν_2 (δ) doubly degenerate bending vibrations of the SO_4 groups. The number of split ν_2 (δ) vibrations is in accordance with the presence of several non-equivalent SO_4 tetrahedra in the structures of all three minerals.

Vibrations of UO_2^{2+}

The bands related to the activated ν_3 antisymmetric stretching vibration of the uranyl ion, $(UO_2)^{2+}$, were observed in the spectra of all three minerals. The reason for activation of this mode in the Raman spectra is the lowering of the factor group

https://doi.org/10.1180/minmag.2016.080.120 Published online by Cambridge University Press

TABLE 6. (*contd*.)

Ottohahnite*

Na1–O17	2.349(4)	Na4–O18	2.343(4)	S1–O1	1.449(4)	Hydrogen bonds	
Na1–O16	2.377(4)	Na4–OW3	2.399(4)	S1–O2	1.452(4)	OW1–O14	2.968(7)
Na1–OW3	2.386(4)	Na4–OW1	2.404(5)	S1–O3	1.455(4)	OW1–O22	3.198(5)
Na1–O20	2.425(4)	Na4–O14	2.406(4)	S1–O4	1.516(4)	OW2–O6	3.053(5)
Na1–OW4	2.439(5)	Na4–O2	2.634(5)	<S1–O>	1.470	OW2–O18	2.842(6)
Na1–O11	2.853(4)	Na4–O14	2.655(5)			OW3–OW6	2.793(6)
Na1–O10	2.867(4)	<Na4–O>	2.474	S2–O5	1.446(4)	OW3–OW7a	2.710(9)
<Na1–O>	2.528			S2–O6	1.457(4)	OW3–OW7b	3.01(2)
		Na5–O1	2.339(4)	S2–O7	1.489(3)	OW4–OW5	2.838(6)
Na2–O3	2.352(5)	Na5–OW7a	2.349(9)	S2–O8	1.489(3)	OW4–OW8	2.739(7)
Na2–O9	2.357(4)	Na5–OW1	2.380(5)	<S2–O>	1.468	OW5–O9	2.839(6)
Na2–O6	2.439(4)	Na5–O19	2.417(4)			OW5–O21	3.064(5)
Na2–O24	2.462(4)	Na5–O13	2.522(5)	S3–O9	1.448(4)	OW6–O17	2.757(5)
Na2–O6	2.486(4)	Na5–OW7b	2.59(3)	S3–O10	1.473(3)	OW6–O23	2.941(5)
Na2–O22	2.615(4)	Na5–O1	2.711(5)	S3–O11	1.476(4)	OW7a–OW8	2.824(10)
<Na2–O>	2.452	Na5–O4	2.897(4)	S3–O12	1.477(4)	OW7a–OW9	2.790(17)
		<Na5–O>	2.527*	<S3–O>	1.469	OW7b–O1	2.93(5)
Na3–OW5	2.375(5)					OW7b–OW8	3.00(3)
Na3–O5	2.385(4)	Na6–OW6	2.306(4)	S4–O13	1.426(4)	OW8–O13	2.773(7)
Na3–O15	2.386(4)	Na6–OW2	2.357(5)	S4–O14	1.449(4)	OW8–OW9	2.931(11)
Na3–OW2	2.403(5)	Na6–OW4	2.384(5)	S4–O15	1.495(3)	OW9–O3	2.867(10)
Na3–O2	2.576(5)	Na6–O2	2.402(5)	S4–O16	1.509(3)	OW9–O9	3.180(10)
Na3–O5	2.846(4)	Na6–O5	2.638(5)	<S4–O>	1.470		
Na3–O8	2.934(4)	Na6–O18	2.885(5)				
Na3–O3	2.961(6)	Na6–O7	2.961(5)	S5–O17	1.441(3)		
<Na3–O>	2.608	<Na6–O>	2.562	S5–O18	1.452(4)		
				S5–O19	1.496(4)		
U1–O21	1.762(4)	U2–O23	1.770(3)	S5–O20	1.500(3)		
U1–O22	1.768(4)	U2–O24	1.779(3)	<S5–O>	1.472		
U1–O8	2.313(3)	U2–O4	2.285(3)				
U1–O11	2.365(3)	U2–O7	2.350(3)				
U1–O12	2.388(3)	U2–O10	2.374(3)				
U1–O15	2.419(3)	U2–O19	2.430(3)				
U1–O16	2.420(3)	U2–O20	2.447(3)				
$<U1–O_{Ur}>$	1.765	$<U2–O_{Ur}>$	1.775				
$<U1–O_{eq}>$	2.381	$<U2–O_{eq}>$	2.377				

*The contributions of Na–OW7a and Na–OW7b to <Na–O> are weighted according to the refined occupancies of the OW7a and OW7b sites.

(symmetry) due to the relatively low symmetry (monoclinic or triclinic) of these minerals. The bands are of low or very low intensity and are observed in the range ~960 to ~920 cm^{-1}. The very strong bands observed at ~830 cm^{-1} are attributed to the ν_1 symmetric stretching vibration of the uranyl ion.

The approximate U–O bond-lengths inferred from the observed energies of the $(UO_2)^{2+}$ vibrations using the empirical relation of Bartlett and Cooney (1989) is 1.79 Å, consistent with the bond-lengths obtained in our X-ray studies (klaprothite ~1.78 Å, péligotite ~1.79 Å, ottohahnite ~1.77 Å) and identical to the most common bond-length given by Burns *et al.* (1997) for the uranyl pentagonal bipyramid, 1.79 Å.

The very weak bands at ~550 and ~500 cm^{-1} may be attributable to the ν ($U–O_{ligand}$) vibrations. Bands of medium intensity at low wavenumbers, ~250 cm^{-1}, can be assigned to the ν_2 (δ) doubly degenerate bending vibrations of $(UO_2)^{2+}$ (e.g. Bullock and Parret, 1970; Ohwada, 1976; Brittain

https://doi.org/10.1180/minmag.2016.080.120 Published online by Cambridge University Press

TABLE 7. Bond-valence analysis for klaprothite, péligotite and ottohahnite. Values are expressed in valence units.*

Klaprothite	Na1	Na2	Na3	Na4	Na5	Na6	Na7	U	S1	S2	S3	S4	H bonds	Σ
O1		0.16			0.04				1.57				0.13	1.90
O2			0.15	0.11			$0.21^{\times 2\downarrow}$		1.54					2.01
O3	0.08								1.54				0.16,0.18	1.96
O4	0.08							0.57	1.39					1.96
O5		0.11								1.60			0.12	1.83
O6	0.14		0.15			$0.15^{\times 2\downarrow}$				1.57				2.01
O7			0.13	0.15						1.54			0.17	1.99
O8						$0.08^{\times 2\downarrow}$		0.61		1.39				2.08
O9	0.21					$0.06^{\times 2\downarrow}$					1.61			1.88
O10		0.12			0.16						1.55		0.16	1.99
O11			0.16	0.19							1.55		0.15	2.05
O12			0.10			$0.15^{\times 2\downarrow}$		0.62			1.33			2.20
O13		0.19			0.13							1.62		1.94
O14			0.23				$0.24^{\times 2\downarrow}$					1.61		2.08
O15	0.17							0.48				1.41		2.06
O16				0.20				0.46				1.39		2.05
O17		0.18						1.71					0.15	2.04
O18	0.14							1.70						1.84
OW1	0.18				0.14								–0.12,–0.15	0.05
OW2			0.12	0.20			$0.04^{\times 2\downarrow}$						–0.15,–0.16	0.05
OW3		0.19			0.16								–0.18,–0.17	0.00
OW4				0.18	0.18								–0.13,–0.16	0.07
Σ	1.00	0.95	1.04	1.03	0.81	0.88	0.98	6.15	6.04	6.10	6.04	6.03		

https://doi.org/10.1180/minmag.2016.080.120 Published online by Cambridge University Press

TABLE 7. (*contd.*)

Péligotite	Na1	Na2	Na3	Na4	Na5	Na6	Na7	U	S1	S2	S3	S4	H bonds	Σ
O1					0.12				1.58				0.12	1.83
O2			0.15	0.13			$0.20^{\times 2\downarrow}$		1.56					2.03
O3	0.04						$0.07^{\times 2\downarrow}$		1.55				0.15,0.17	1.98
O4	0.03							0.60	1.44					2.07
O5		0.17								1.59			0.14	1.90
O6	0.13		0.19			$0.12^{\times 2\downarrow}$				1.57				2.01
O7			0.04	0.16						1.55			0.15	1.90
O8						$0.11^{\times 2\downarrow}$		0.63		1.35				2.09
O9	0.23					$0.12^{\times 2\downarrow}$					1.58			1.93
O10		0.22,0.16									1.57			1.96
O11			0.13	0.21							1.55		0.14	2.03
O12			0.10			$0.14^{\times 2\downarrow}$		0.58			1.33			2.15
O13			0.22		0.25,0.17							1.61		2.04
O14							$0.22^{\times 2\downarrow}$					1.64		2.08
O15	0.19							0.48				1.42		2.09
O16				0.17				0.47				1.38		2.01
O17		0.17			0.13			1.67						1.97
O18	0.16							1.72						1.88
OW1	0.21	0.11											–0.12	0.19
OW2			0.15	0.15									–0.14,–0.15	0.01
OW3		0.19			0.21								–0.17,–0.15	0.08
OW4				0.20	0.08								–0.14	0.14
Σ	1.00	1.03	0.98	1.00	0.98	0.98	0.97	6.15	6.13	6.06	6.04	6.04		

TABLE 7. (*contd.*)

Ottohahnite	Na1	Na2	Na3	Na4	Na5	Na6	U1	U2	S1	S2	S3	S4	S5	H bonds	Σ
O1					0.21,0.08				1.60					+0.05	1.94
O2			0.11	0.09		0.17			1.59						1.96
O3		0.20	0.04						1.58					+0.08	1.90
O4					0.05			0.64	1.34						2.03
O5			0.18,0.05			0.09				1.62					1.94
O6		0.16,0.14								1.57				+0.12	1.99
O7						0.04		0.56		1.44					2.04
O8			0.04				0.60			1.44					2.08
O9		0.20									1.61			+0.17,+0.05	2.03
O10	0.05							0.54			1.50				2.09
O11	0.05						0.55				1.49				2.09
O12							0.52				1.49				2.01
O13					0.13							1.71		+0.20	2.04
O14				0.17,0.09								1.60		+0.14	2.00
O15			0.18				0.49					1.42			2.09
O16	0.19						0.49					1.36			2.04
O17	0.20												1.64	+0.20	2.04
O18				0.20		0.05							1.59	+0.17	2.01
O19					0.17			0.48					1.41		2.06
O20	0.16							0.47					1.40		2.03
O21							1.75							+0.12	1.87
O22		0.10					1.73							+0.10	1.93
O23								1.72						+0.14	1.86
O24		0.15						1.69							1.84
OW1				0.17	0.19									–0.14,–0.10	0.12
OW2			0.17			0.23								–0.12,–0.17	0.11
OW3	0.18			0.18										–0.19,–0.19	–0.02
OW4	0.16					0.18								–0.17,–0.21	–0.04
OW5			0.19											+0.17,–0.17, –0.12	0.07
OW6						0.23								+0.19,–0.20, –0.14	0.08

TABLE 7. (*contd.*)

Ottohahnite	Na1	Na2	Na3	Na4	Na5	Na6	U1	U2	S1	S2	S3	S4	S5	H bonds	Σ
OW7					0.14,0.03									+0.19,–0.25, –0.09	0.02
OW8														+0.21,+0.16, –0.20,–0.15	0.02
OW9														+0.13,+0.15, –0.16,–0.10	0.02
Σ	0.99	0.95	0.96	0.90	1.00	0.99	6.13	6.10	6.11	6.07	6.09	6.09	6.04		

*S^{6+}–O bond strength from Brown and Altermatt (1985); Na^{+}–O bond strength from Wood and Palenik (1999); U^{6+}–O bond strength from Burns *et al.* (1997); hydrogen-bond strengths based on O–O bond lengths from Ferraris, G. and Ivaldi, G. (1988).

et al., 1985; Plášil *et al.*, 2010, 2015). Weak Raman bands at ~150 cm^{-1} are attributed to $–O_{eq}–U–O_{eq}–$ bending vibrations (Ohwada, 1976).

Vibrations of Na–O bonds and lattice modes

Weak Raman bands with shoulders at ~280 cm^{-1} could be related to Na–O stretching vibrations or to the ν ($U–O_{ligand}$) stretching vibration (Plášil *et al.*, 2010, 2015). The bands located below 100 cm^{-1} are related to the lattice modes.

Composition

Chemical analyses of klaprothite, péligotite and ottohahnite were performed using a CamScan 4D electron microprobe in energy-dispersive spectroscopy (EDS) mode (20 kV, 500 pA and beam rasterized on an area 8 μm × 8 μm in order to minimize sample damage). The EDS mode with the above experimental conditions, rather than wavelength-dispersive spectroscopy (WDS) mode, was chosen because of the instability of these minerals under the electron beam caused by the high contents of both Na and H_2O. Attempts to use the WDS mode with higher beam current were unsuccessful because of significant decomposition of the minerals after several seconds under the electron beam. Standards used were chkalovite for Na, synthetic UO_2 for U and synthetic ZnS for S. H_2O was not determined directly because of the scarcity of pure material. The H_2O content was calculated by stoichiometry on the basis of the number of O apfu from crystal-structure determinations. The Raman spectra confirm the presence of H_2O groups and the absence of B–O, C–O and N–O bonds in the minerals. No other elements with atomic numbers higher than 8 were observed. Analytical data are given in Table 2.

The empirical formula of klaprothite, calculated as the mean of 11 representative spot analyses, is $Na_{6.01}(U_{1.03}O_2)(S_{0.993}O_4)_4(H_2O)_4$ and that of péligotite, calculated as the mean of 8 analyses, is $Na_{5.82}(U_{1.02}O_2)(S_{1.003}O_4)_4(H_2O)_4$, both based on 22 O apfu). The ideal formula for both minerals is $Na_6(UO_2)(SO_4)_4(H_2O)_4$ which requires Na_2O 21.51, UO_3 33.10, SO_3 37.05 and H_2O 8.34, total 100 wt.%. The empirical formula of ottohahnite, calculated as the mean of 12 analyses, is $Na_{5.88}(U_{0.99}O_2)_2(S_{1.008}O_4)_5(H_2O)_{8.5}$ based on 32.5 O apfu. Its ideal formula is $Na_6(UO_2)_2(SO_4)_5(H_2O)_7 \cdot 1.5H_2O$, which requires Na_2O 14.18, UO_3 43.62, SO_3 30.52 and H_2O 11.68, total 100 wt.%.

https://doi.org/10.1180/minmag.2016.080.120 Published online by Cambridge University Press

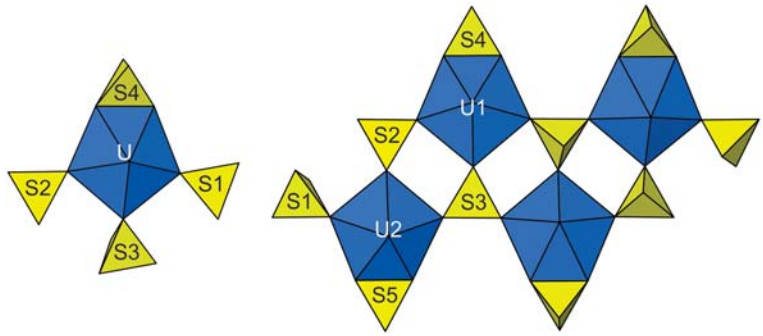

FIG. 7. (*Left*) The $[(UO_2)(SO_4)_4]^{6-}$ cluster in the structures of klaprothite and péligotite. (*Right*) The $[(UO_2)_4(SO_4)_{10}]^{12-}$ cluster constructed of four linked $[(UO_2)(SO_4)_4]^{6-}$ clusters.

The Gladstone-Dale compatibility index $1 - (K_P/K_C)$ for the empirical formulas of klaprothite, péligotite and ottohahnite are –0.008 (superior), –0.015 (superior) and –0.021 (excellent), respectively (Mandarino, 2007). As noted by Kampf *et al.* (2015*c*), Gladstone-Dale calculations for uranyl sulfates should utilize $k(UO_3) = 0.118$, as provided by Mandarino (1976).

X-ray crystallography and structure refinement

Powder X-ray studies were carried out using a Rigaku R-Axis Rapid II curved imaging plate microdiffractometer, with monochromatized Mo*K*α radiation (λ = 0.71075 Å). A Gandolfi-like motion on the φ and ω axes was used to randomize the orientation of the sample and observed *d*-values and intensities were derived by profile fitting using *JADE 2010* software (Materials Data, Inc.). The powder data presented in Table 3 show good agreement with the patterns calculated from the structure determinations. Unit-cell parameters refined from the powder data using *JADE 2010* with whole pattern fitting are for klaprothite: $a = 9.812(4)$, $b = 9.739(4)$, $c = 20.855(4)$ Å, $\beta = 98.743(8)°$ and $V = 1969.7(12)$ Å^3; for péligotite: $a = 9.811(9)$, $b = 9.928(10)$, $c = 10.635(10)$ Å, $\alpha = 88.79(3)°$, $\beta = 74.00(3)°$, $\gamma = 89.27(2)°$ and $V = 995.5(17)$ Å^3; and for ottohahnite: $a = 9.979(8)$, $b = 11.660(8)$, $c = 14.277(8)$ Å, $\alpha = 113.48(3)°$, $\beta = 104.29(2)°$, $\gamma = 91.35(2)°$ and $V = 1462.6(18)$ Å^3.

The single-crystal structure data for klaprothite, péligotite and ottohahnite were collected at room temperature on a Rigaku R-Axis Rapid II curved imaging plate microdiffractometer, also using monochromatized Mo*K*α radiation. The data were processed using the Rigaku *CrystalClear* software package and empirical (multi-scan) absorption corrections were applied using the *ABSCOR* program (Higashi, 2001) in the *CrystalClear* software suite. The structures were solved by direct methods using *SIR2011* (Burla *et al.*, 2012). *SHELXL-2013* (Sheldrick, 2008) was used for the refinement of the structures. Difference-Fourier syntheses located all H atom positions in the structures of klaprothite and péligotite; however, H atom positions could not be located in the ottohahnite structure. For klaprothite and péligotite, H atom positions were refined with soft restraints of 0.82(3) Å on the O–H distances and 1.30(3) Å on the H–H distances and with the U_{eq} of each H set to 1.2 times that of its donor O atom.

For the structures of both klaprothite and péligotite, all non-hydrogen atoms refined to full occupancy, although the Na7 sites, at centres of symmetry in both structures, exhibited significant displacement along **a**. Refining these as split sites improved the *R*-factors slightly, but it was ultimately decided to report them as unsplit sites. The same high displacement along **a** is noted for this site in the structure of the synthetic phase equivalent to klaprothite (Plášil *et al.*, 2015). For the structure of ottohahnite, all sites were refined with full occupancy except for three O sites in relatively close proximity: The occupancies of OW7a and OW7b (1.18 Å apart and coordinated to Na5) refined to 0.74 and 0.37. The occupancy of OW9 (1.77 Å from OW7b and not coordinated to a cation) refined to 0.48. In the final refinement, the OW7a and OW7b sites were constrained to a total occupancy of 1 and the OW9 site was assigned an occupancy of 0.5.

https://doi.org/10.1180/minmag.2016.080.120 Published online by Cambridge University Press

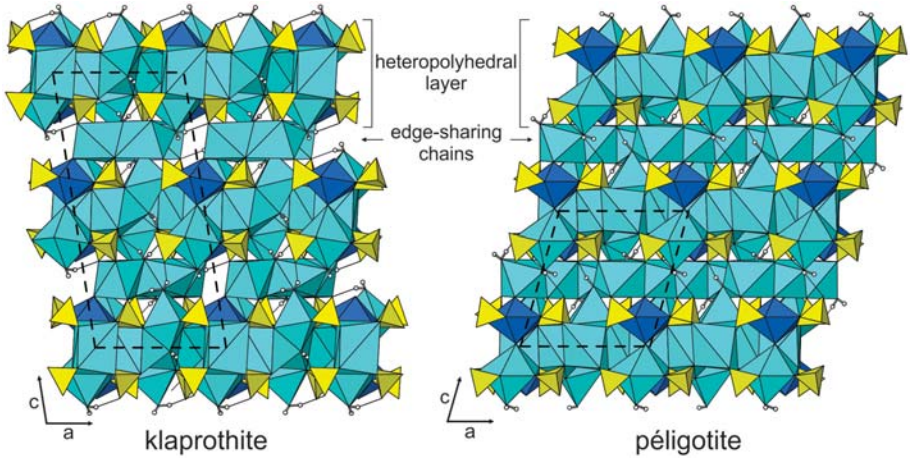

FIG. 8. The structures of klaprothite and péligotite viewed along [010]. Na polyhedra are turquoise blue. Unit-cell outlines are shown as dashed lines.

Data collection and refinement details are given in Table 4, atom coordinates and displacement parameters in Table 5, selected bond distances in Table 6 and bond-valence analyses in Table 7.

Description and discussion of the structures

In the structures of klaprothite, péligotite and ottohahnite, the U sites are surrounded by seven O atom sites forming squat pentagonal bipyramids. This is the most typical coordination for U^{6+},

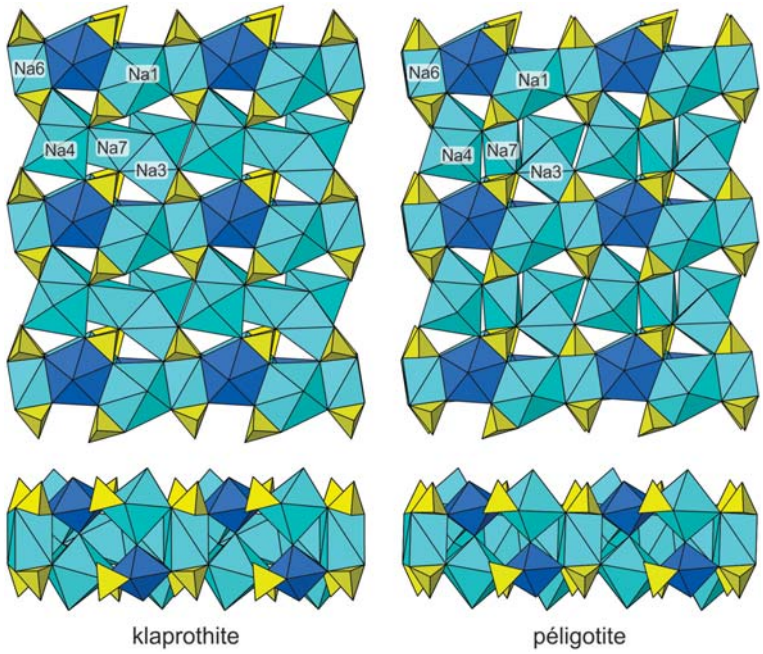

FIG. 9. Heteropolyhedral layers in the structures of klaprothite and péligotite viewed perpendicular to {001} (upper images) and along [100] (lower images); [010] is horizontal in all cases.

https://doi.org/10.1180/minmag.2016.080.120 Published online by Cambridge University Press

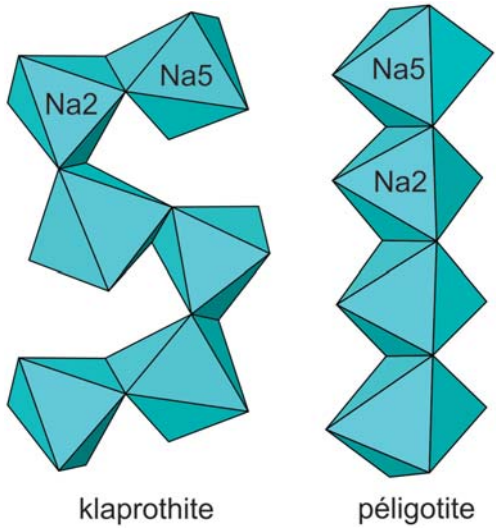

FIG. 10. Edge-sharing chains of NaO6 octahedra in the structures of klaprothite and péligotite. The chain in klaprothite is along [010] and that in péligotite is along [110].

particularly in uranyl sulfates (Krivovichev, 2010, 2013), where the two short apical bonds of the bipyramid constitute the uranyl group. The bond lengths in U^{6+}-coordination polyhedron in all three structures (klaprothite: $\langle U1–O_{ap}\rangle = 1.775$, $\langle U1–O_{eq}\rangle = 2.368$ Å; péligotite: $\langle U1–O_{ap}\rangle = 1.777$, $\langle U1–O_{eq}\rangle = 2.364$ Å; ottohahnite: $\langle U1–O_{ap}\rangle = 1.765$, $\langle U1–O_{eq}\rangle = 2.381$, $\langle U2–O_{ap}\rangle = 1.775$, $\langle U2–O_{eq}\rangle = 2.377$ Å) are consistent with the most typical lengths observed for [7]-coordinated U^{6+} (Burns *et al.*, 1997). In all three structures, all five of the equatorial O atoms also participate in SO_4 tetrahedra and, in each case, three of the SO_4 tetrahedra share single equatorial O atoms and one shares two equatorial O atoms, i.e. a shared polyhedral edge. Such a bidentate linkage between a UO_7 pentagonal bipyramid and a SO_4 tetrahedron has previously been reported in synthetic phases, but never in minerals. The $[(UO_2)(SO_4)_4]^{6-}$ uranyl sulfate cluster (Fig. 7) is the fundamental building block in the structures of klaprothite and péligotite; while in the structure of ottohahnite, four of these uranyl-sulfate clusters are combined through shared SO_4 tetrahedra to form a larger $[(UO_2)_4(SO_4)_{10}]^{12-}$ cluster (Fig. 7). Among synthetic Na uranyl sulfates, the structure of the synthetic equivalent of klaprothite was reported by Plášil *et al.* (2015) and the same $[(UO_2)(SO_4)_4]^{6-}$ cluster with a bidentate U–S linkage was reported in the structures of $Na_{10}[(UO_2)(SO_4)_4](SO_4)_2{\cdot}3H_2O$ (Burns and Hayden, 2002), $KNa_5[(UO_2)(SO_4)_4](H_2O)$ (Hayden and Burns, 2002*a*) and $Na_6(UO_2)(SO_4)_4(H_2O)_2$ (Hayden and Burns, 2002*b*). The $[(UO_2)_4(SO_4)_{10}]^{12-}$ cluster in the structure of ottohahnite has not previously been reported in the structure of any mineral or synthetic phase.

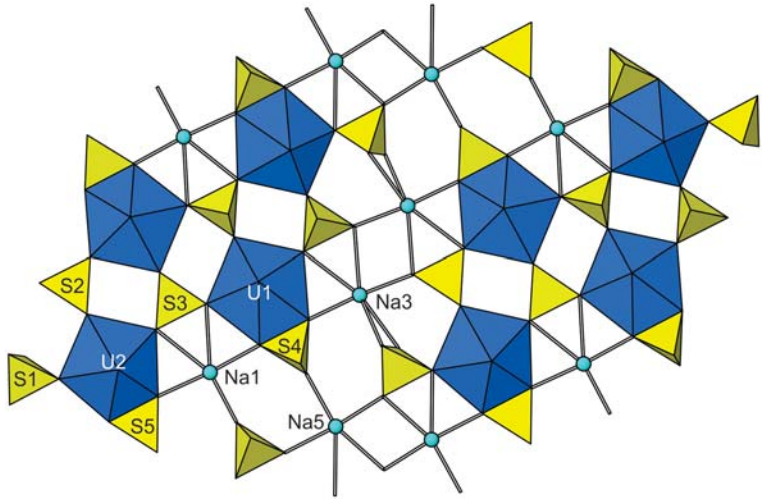

FIG. 11. One slice parallel to $\{11\bar{2}\}$ in the structure of ottohahnite containing the $[(UO_2)_4(SO_4)_{10}]^{12-}$cluster and Na1, Na3 and Na5 atoms. Na–O bonds are shown as sticks.

https://doi.org/10.1180/minmag.2016.080.120 Published online by Cambridge University Press

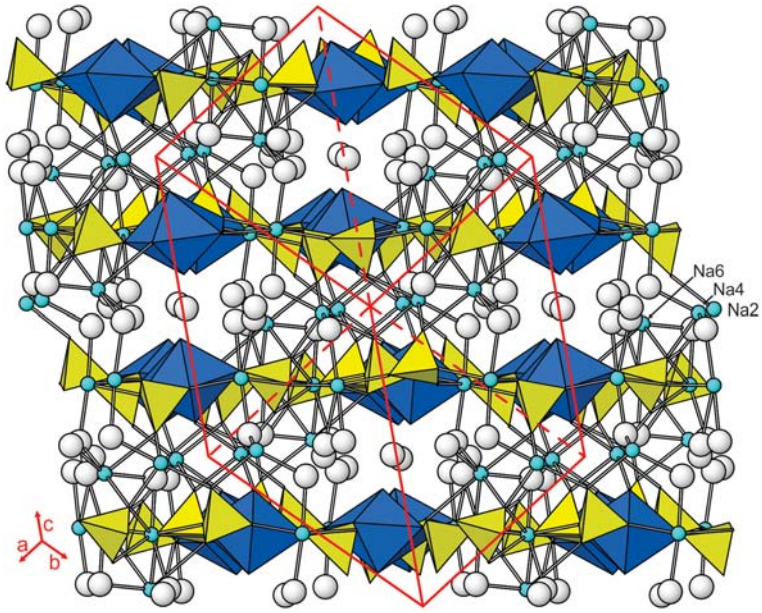

FIG. 12. The structure ottohahnite viewed down [111] with $\{11\bar{2}\}$ horizontal. O atoms of H_2O groups are shown as white spheres. The unit cell outline is shown in red.

In the structures of klaprothite and péligotite, seven Na sites, in 6-, 7- and 8-coordinations, link to the O atoms in the clusters and to four H_2O groups, yielding relatively loosely bonded frameworks (Fig. 8). In both structures, the $Na1O_7$, $Na3O_7$, $Na4O_6$, $Na6O_8$ and $Na7O_6$ polyhedra combine with the uranyl sulfate clusters forming more tightly bonded heteropolyhedral layers parallel to {001} in which the Na polyhedra share some faces and edges with one another, and edges and corners with the UO_7 and SO_4 polyhedra of the uranyl sulfate clusters. The polyhedral layers in the two structures (Fig. 9) are topologically identical except for a minor difference in the $Na7O_6$ coordination. The principal difference between the structures is the configuration of the $Na2O_6$ and $Na5O_6$ octahedra between the layers. These octahedra form a zig-zag edge-sharing chain parallel to [010] in the structure of klaprothite, while in the structure of péligotite they form a straight edge-sharing chain parallel to [110] (Fig. 10).

In the structure of ottohahnite, the $[(UO_2)_4(SO_4)_{10}]^{12-}$ clusters are linked to one another *via* bonds to six different Na atoms. The Na atoms, with coordinations ranging from 6 to 8, bond to O atoms in the clusters and to H_2O groups. There are seven different H_2O groups (one of which is split) bonded to Na atoms and two H_2O groups, one of which is half occupied, bonded only though hydrogen bonds. The plane of the $[(UO_2)_4(SO_4)_{10}]^{12-}$ cluster is parallel to $\{11\bar{2}\}$. Na1, Na3 and Na5 are in approximately the same plane with the cluster. Figure 11 shows the linkages between the clusters and $Na1O_7$, $Na3O_8$ and $Na5O_7$ coordinations within one slice through the structure parallel to $\{11\bar{2}\}$. The Na2, Na4 and Na6 atoms are placed between these slices linking them together via Na–O bonds and yielding $Na2O_6$, $Na4O_6$ and $Na6O_7$ coordinations. The isolated H_2O groups (OW8 and OW9) are also sandwiched in between the slices (Fig. 12).

Acknowledgements

Structures Editor Peter Leverett and an anonymous reviewer are thanked for their comments on the manuscript. Atali A. Agakhanov and Ladislav Lapčák are thanked for their assistance with the chemistry and Raman measurements, respectively. A portion of this study was funded by the John Jago Trelawney Endowment to the Mineral Sciences Department of the Natural History Museum of Los Angeles County. This research was also financially supported by GACR post-doctoral Grant no. 13-31276P to J.P. and by the Ministry of Culture of the Czech Republic (DKRVO 2016/02; National Museum 00023272) to J.Č.

https://doi.org/10.1180/minmag.2016.080.120 Published online by Cambridge University Press

References

Bartlett, J.R. and Cooney, R.P. (1989) On the determination of uranium-oxygen bond lengths in dioxouranium(VI) compounds by Raman spectroscopy. *Journal of Molecular Structure*, **193**, 295–300.

Brown, I.D. and Altermatt, D. (1985) Bond-valence parameters from a systematic analysis of the inorganic crystal structure database. *Acta Crystallographica*, **B41**, 244–247.

Brittain, H.G., Ansari, P., Toivonen, J., Niinisto, L., Tsao, L. and Perry, D.L. (1985) Photophysical Studies of Uranyl Complexes. VIII. Luminiscence Spectra of $UO_2SO_4 \cdot 31/2H_2O$ and Two Polymorphs of Bis(urea) Uranyl Sulfate. *Journal of Solid State Chemistry*, **59**, 259–264.

Bullock, H. and Parret, F.W. (1970) The low frequency infrared and Raman spectroscopic studies of some uranyl complexes: the deformation frequency of the uranyl ion. *Canadian Journal of Chemistry*, **48**, 3095–3097.

Burla, M.C., Caliandro, R., Camalli, M., Carrozzini, B., Cascarano, G.L., Giacovazzo, C., Mallamo, M., Mazzone, A., Polidori, G. and Spagna, R. (2012) *SIR2011*: a new package for crystal structure determination and refinement. *Journal of Applied Crystallography*, **45**, 357–361.

Burns, P.C. and Hayden, L.A. (2002) A uranyl sulfate cluster in $Na_{10}[(UO_2)(SO_4)_4](SO_4)_2 \cdot 3H_2O$. *Acta Crystallographica*, **C58**, i121–i123.

Burns, P.C., Ewing, R.C. and Hawthorne, F.C. (1997) The crystal chemistry of hexavalent uranium: polyhedron geometries, bond-valence parameters, and polymerization of polyhedra. *The Canadian Mineralogist*, **35**, 1551–1570.

Chenoweth, W.L. (1993) *The Geology and Production History of the Uranium Deposits in the White Canyon Mining District, San Juan County, Utah*. Utah Geological Survey Miscellaneous Publication, 93–3.

Ferraris, G. and Ivaldi, G. (1988) Bond valence vs. bond length in O···O hydrogen bonds. *Acta Crystallographica*, **B44**, 341–344.

Hawthorne, F.C. (2012) A bond-topological approach to theoretical mineralogy: crystal structure, chemical composition and chemical reactions. *Physics and Chemistry of Minerals*, **39**, 841–874.

Hawthorne, F.C. and Schindler, M. (2008) Understanding the weakly bonded constituents in oxysalt minerals. *Zeitschrift für Kristallographie*, **223**, 41–68.

Hayden, L.A. and Burns, P.C. (2002*a*) The sharing of an edge between a uranyl pentagonal bipyramid and sulfate tetrahedron in the structure of $KNa_5[(UO_2)(SO_4)_4](H_2O)$. *The Canadian Mineralogist*, **40**, 211–216.

Hayden, L.A. and Burns, P.C. (2002*b*) A novel uranyl sulfate cluster in the structure of $Na_6(UO_2)(SO_4)_4(H_2O)_2$. *Journal of Solid State Chemistry*, **163**, 313–318.

Higashi, T. (2001) *ABSCOR*. Rigaku Corporation, Tokyo.

Kampf, A.R., Plášil, J., Kasatkin, A.V. and Marty, J. (2014) Belakovskiite, $Na_7(UO_2)(SO_4)_4(SO_3OH)(H_2O)_3$, a new uranyl sulfate mineral from the Blue Lizard mine, San Juan County, Utah, USA. *Mineralogical Magazine*, **78**, 639–649.

Kampf, A.R., Kasatkin, A.V., Čejka, J. and Marty, J. (2015*a*) Plášilite, $Na(UO_2)(SO_4)(OH) \cdot 2H_2O$, a new uranyl sulfate mineral from the Blue Lizard mine, San Juan County, Utah, USA. *Journal of Geosciences*, **60**, 1–10.

Kampf, A.R., Plášil, J., Kasatkin, A.V. and Marty, J. (2015*b*) Bobcookite, $NaAl(UO_2)_2(SO_4)_4(H_2O)_{18}$, and wetherillite, $Na_2Mg(UO_2)_2(SO_4)_4 \cdot 18H_2O$, two new uranyl sulfate minerals from the Blue Lizard mine, San Juan County, Utah, USA. *Mineralogical Magazine*, **79**, 695–714.

Kampf, A.R., Plášil, J., Kasatkin, A.V., Marty, J. and Čejka, J. (2015*c*) Fermiite, $Na_4(UO_2)(SO_4)_3 \cdot 3H_2O$, and oppenheimerite, $Na_2(UO_2)(SO_4)_2 \cdot 3H_2O$, two new uranyl sulfate minerals from the Blue Lizard mine, San Juan County, Utah, USA. *Mineralogical Magazine*, **79**, 1123–1142.

Kampf, A.R., Plášil, J., Čejka, J., Marty, J., Škoda, R. and Lapčák, L. (2017*a*) Alwilkinsite-(Y), a new rare-earth uranyl sulfate mineral from the Blue Lizard mine, San Juan County, Utah, USA. *Mineralogical Magazine*, **81**, https:doi.org/10.1180/minmag.2016.080.139.

Kampf, A.R., Plášil, J., Kasatkin, A.V., Marty, J. Čejka, J. and Ladislav Lapčák (2017*b*) Shumwayite, $[(UO_2)(SO_4)(H_2O)_2]_2 \cdot H_2O$, a new uranyl sulfate mineral from Red Canyon, San Juan County, Utah, USA. *Mineralogical Magazine*, **81**, 273–285.

Krivovichev, S.V. (2010) Actinyl compounds with hexavalent elements (S, Cr, Se, Mo) – structural diversity, nanoscale chemistry, and cellular automata modeling. *European Journal of Inorganic Chemistry*, **2010**, 2594–2603.

Krivovichev, S.V. (2013) Crystal chemistry of uranium oxides and minerals. Pp. 611–640 in: *Comprehensive Inorganic Chemistry II, Vol 2* (J. Reedijk and K. Poeppelmeier, editors). Elsevier, Oxford, UK.

Libowitzky, E. (1999) Correlation of O–H stretching frequencies and O–H···O hydrogen bond lengths in minerals. *Monatshefte für Chemie*, **130**, 1047–1059.

Mandarino, J.A. (1976) The Gladstone-Dale relationship – Part 1: derivation of new constants. *The Canadian Mineralogist*, **14**, 498–502.

Mandarino, J.A. (2007) The Gladstone–Dale compatibility of minerals and its use in selecting mineral species for further study. *The Canadian Mineralogist*, **45**, 1307–1324.

Ohwada, K. (1976) Infrared spectroscopic studies of some uranyl nitrate complexes. *Journal of Coordination Chemistry*, **6**, 75–80.

Plášil, J., Buixaderas, E., Čejka, J., Sejkora, J., Jehlička, J. and Novák, M. (2010) Raman spectroscopic study of the uranyl sulphate mineral zippeite: low wavenumber and U–O stretching regions. *Analytical and Bioanalytical Chemistry*, **397**, 2703–2715.

https://doi.org/10.1180/minmag.2016.080.120 Published online by Cambridge University Press

Plášil, J., Kampf, A.R., Kasatkin, A.V., Marty, J., Škoda, R., Silva, S. and Čejka, J. (2013) Meisserite, $Na_5(UO_2)(SO_4)_3(SO_3OH)(H_2O)$, a new uranyl sulfate mineral from the Blue Lizard mine, San Juan County, Utah, USA. *Mineralogical Magazine*, **77**, 2975–2988.

Plášil, J., Kampf, A.R., Kasatkin, A.V. and Marty, J. (2014) Bluelizardite, $Na_7(UO_2)(SO_4)_4Cl(H_2O)_2$, a new uranyl sulfate mineral from the Blue Lizard mine, San Juan County, Utah, USA. *Journal of Geosciences*, **59**, 145–158.

Plášil, J., Meisser, N. and Čejka, J. (2015) The crystal structure of $Na_6[(UO_2)(SO_4)_4](H_2O)_4$: X-ray and Raman spectroscopy study. *The Canadian Mineralogist*, **54**, 5–20.

Sheldrick, G.M. (2008) A short history of *SHELX*. *Acta Crystallographica*, **A64**, 112–122.

Wood, R.M. and Palenik, G.J. (1999) Bond valence sums in coordination chemistry. Sodium-oxygen complexes. *Inorganic Chemistry*, **38**, 3926–3930.

https://doi.org/10.1180/minmag.2016.080.120 Published online by Cambridge University Press